THE CRITICAL ASSESSMENT OF TERNARY ALLOY PHASE DIAGRAM DATA

Alan Prince

The assessment of published data on ternary alloy phase diagrams is concerned with:

1 examination of the validity of the experimental techniques used to generate the data, and

2 confirmation that the data obeys the laws of heterogeneous equilibria and that a consistent interpretation of the data emerges.

This contribution concentrates on the second aspect of the assessment process. Consideration is given to the critical assessment of published data in terms of:

a liquidus surfaces,

b surfaces of secondary separation,

c vertical sections,

d isothermal sections,

e the designation of phase regions.

a Liquidus Surfaces

Detailed surveys of ternary systems include projections of the liquidus surface with isotherms, monovariant curves and invariant reaction points. The projection of the monovariant curves and their intersection at invariant points should be consistent with the associated binary invariant reactions and the Phase Rule. An example where this consistency was absent is illustrated in Figure 1. It will be noted that no ternary monovariant curves are associated with the binary invariant reactions p_1 (system A-B) or p_3 (system A-C). Furthermore the monovariant curves associated with the binary invariant reactions e_1, e_2 and e_3 cannot meet within the ternary in the manner shown in Figure 1. Such a construction implies the equilibrium of six phases at the invariant point U - liquid + (A) + A_2C + AC + (C) + B_3C. The Phase Rule dictates that invariant reactions in isobaric sections

of ternary systems involve four phases only. Finally the monovariant curve p_3p_2 implies a continuous series of solid solutions between the phases B_3C and β. This may be correct but, in view of the other errors, it should be viewed with suspicion.

It is rare for refereed papers to be published with such glaring errors. The more normal difficulty in assessing ternary reaction equilibria is that the ternary data is frequently older data and this data has to be assessed in terms of more modern binary data. Modern work that leads to the revision of the older binary data in terms of a shift in liquidus temperatures and in the previously accepted binary invariant reaction points can be used in the assessment of the older ternary data. In general the ternary data is constrained to fit the modern binary data. However, real difficulties arise when the recent binary data requires more drastic revision of the previously accepted binary phase diagram. For example any ternary system Au-Pb-Me that relied on the Au-Pb phase diagram in Hansen would be incorrect. The discovery of a third stable compound, $AuPb_3$, in the Au-Pb system requires its presence in the ternary equilibria of systems Au-Pb-Me. In the limit the assessor may be left with no choice but to state that the ternary data makes no allowance for the presence of the phase $AuPb_3$ in such systems but it is preferable to apply intelligent speculation in such cases. Some guidance is then given to the reader on the likely reactions involving $AuPb_3$ but it should be made clear in the text of the assessment that the section is speculative and not based on experimental data. The ideal solution is to resolve the matter by further experimental work on the ternary system. Indeed it can be argued that the assessment of ternary alloy phase diagram data frequently requires the carrying out of a few experiments on critical alloy compositions identified as such during the assessment of the published data.

It so happens that the binary system A-C, Figure 1, has been revised by recent work and the ternary system A-B-C defined. Figure 2 shows the projection of the monovariant reactions on to the concentration triangle and identifies seven ternary invariant reactions and two pseudobinary sections in a self-consistent manner.

One advantage of the older ternary publications compared with their modern counterparts is in the tabulation of thermal analysis data for the alloys studied. This is a great help to the assessor since it allows replotting

of the data in a form which may be of more use in the interpretation of the data. An example of this arose in a paper in which the authors tabulated liquidus temperatures, temperatures for secondary separation and for final solidification. No liquidus projection was given by the authors, only a series of vertical sections at constant % A, Figure 3(a). The ternary equilibria is a simple three-phase monovariant eutectic equilibrium represented by the curve e_1e_2, Figure 4. Components A and B are mutually soluble whereas the binary systems A-C and B-C are simple eutectic-type. There is extremely limited solid solubility of both A and B in component C. The authors' presentation of the data by vertical sections at constant % A would be reasonable in normal circumstances since such sections would locate the monovariant eutectic curve e_1e_2. In this case however the data determined by the authors only covered alloys containing $\geqslant$ 30% C. The section at 10% A, Figure 3a, shows a smoothed plot of the data beyond 30% C. Below this level the course of the curves for the liquidus etc are conjectural; they are represented by dashed lines. It is not possible to determine the composition nor the temperature at which the 10% A section intersects the eutectic valley e_1e_2. By taking the tabulated data vertical sections can be constructed for alloys whose compositions lie along lines radiating from the C corner to the A-B binary edge, i e at constant ratios of A : B. The significant point to note is that the surface of secondary separation, where liquid becomes saturated with solid solution A/B and component C, is horizontal because of the virtual insolubility of A/B in C. This allows an assessment of the temperature at which the section, Figure 3(b), cuts the eutectic valley e_2. It does not allow prediction of the composition of the monovariant eutectic liquid. An estimate of composition may be made and liquidus isotherms generated for the complete ternary system. Only the isotherms based on the experimental data are drawn in full; it is prudent to indicate the estimated nature of the isotherms for C $\leqslant$ 30% by dashed lines.

In passing it should be noted (J E Ricci, The Phase Rule and Heterogeneous Equilibrium, page 243) that the projection of monovariant curves which meet at an invariant point are such that there is no angle $> 180^{\circ}$ between the adjacent curves.

It should be self-evident that liquidus isotherms should be drawn to be consistent with the invariant reaction temperatures in the ternary system.

It occasionally happens that liquidus isotherms are in conflict with a stated invariant reaction temperature such that a 750°C reaction is quoted in the text but the liquid composition is placed between the 600°C and 700°C isotherms in the drawing of the liquidus projection. In each ternary assessment it is necessary to check all the data provided by the authors for complete self-consistency. Liquidus isotherms, the trace of monovariant curves, the location of invariant points, the vertical and isothermal sections should all be consistent with each other in the final assessment.

b Surfaces of Secondary Separation

The importance of surfaces of secondary separation in the assessment process can be illustrated by reference to a simple ternary eutectic system with no solid state solubility of the components. A section I - II through the ternary system, Figure 5a, is shown in Figure 5b. An alloy of composition d, on cooling from the melt, will separate primary A until the composition of the liquid meets the monovariant curve e_2E at point d^1. At this temperature, T, the liquid is doubly saturated - with both A and B. An alloy of composition d at a temperature T lies on the surface of secondary separation of A + B from the liquid. The point d, Figure 5b, is equivalent to point d^1 in Figure 5a. Similarly alloy g at temperature T will interest the monovariant curve e_3E at the point g^1, Figure 5a. Of particular interest are alloys of composition corresponding to points e and f, Figure 5b. Alloy e will begin to separate A + C when the liquid composition meets curve e_1E at point e^1. Alloy f will also separate A + C when the liquid composition meets e_1E at point f^1. Points e_1 and f^1 coincide. As points d^1, e^1, and f^1 all lie at the same temperature T the isotherm at T can be drawn in Figure 5a from the data in Figure 5b.

It is normal practice to use the traces of the liquidus surfaces to plot isotherms, i e to use curves hb and ib, Figure 5b. By utilising the surfaces of secondary separation plotted in vertical sections a check can be made for consistency of the published data since:-

a a series of sections similar to Figure 5b at constant % B will give a series of intersection points such as e^1/f^1. They also give a series of points such as b representing the intersection of two

regions of primary solidification. All these points should produce a smooth monovariant curve running from the binary invariant point e_1 to the ternary eutectic point E.

b a series of sections at constant % B or other types of vertical sections will allow a check on the liquidus isotherms presented by the author. Sections such as Figure 5b provide information on the temperatures associated with points on the portion bE of the monovariant curve e_1E, Figure 5a. In theory they also provide temperatures associated with the whole of the monovariant curves e_2E and e_3E but the number of experimental points on the portion I-a of the section I - II, Figure 5b, is likely to be small and the accuracy of extrapolation of points d and g to d^1 and g^1 will be less than for points e and f. A section at a constant % B between e^1/f^1 and E would produce, Figure 5c, confirmatory liquidus compositions at points k and l and compositions on the surface of secondary separation denoted by points j and m. Points A, d and j should lie on a straight line as should points C, g and m.

It is often difficult to determine experimentally the temperature at which secondary separation occurs. This can be associated with undercooling effects, nucleation difficulties or small amounts of separation of the second solid phase. Checks of the liquidus curves against those of secondary separation in vertical sections will often lead to the amendment of the latter.

Surfaces of secondary separation have been considered using a simple ternary eutectic system. They are of equal use in other ternary invariant reactions. Figure 6a is an example of a system containing the reaction $l + C \rightleftharpoons B + X$ and Figure 6b is a section I - II through the system. Isotherms at temperatures T_1, T_2 and T_3 have been sketched in based on the single vertical section. Note that Cy and Xx when extrapolated should meet at the same point on curve pU; Ca and Xb when extrapolated should also meet at the same point on pU.

c Vertical Sections

Use has been made of vertical sections in the consideration of the information to be gained from surfaces of secondary separation. Although not favoured by some experimentalists vertical sections are useful for determining:

1 the ternary liquidus,

2 the course of the monovariant curves,

3 the presence of ternary invariant reactions and the temperature of reaction,

4 the composition of the liquid associated with invariant reactions.

Where authors present a series of vertical sections the assessor should derive from them a series of isothermal sections to ensure consistency between the vertical sections. This procedure will often highlight suspect data on specific vertical sections which must then be amended to produce overall agreement between the various sections. The checking of the curves of monovariant equilibrium has been considered in the previous section. It is obvious that vertical sections provide evidence of invariant reactions since horizontal reaction lines will occur in such sections. The variation of the composition range over which an invariant reaction occurs in different vertical sections is an important parameter to check. In Figure 6a vertical sections at constant % B will show intersection with the four-phase plane BUXC as points on the tie lines XU or BU. If the extremities of the four-phase plane for different vertical sections do not lie on a straight line the data should be amended to produce the most probable tie line (XU and BU). The intersection of tie lines XU and BU gives the composition of the liquid phase involved in the ternary invariant reaction.

Similarly the ternary eutectic point E, Figure 5a, can be obtained as the point of intersection of tie lines such as AaE and CcE. The composition deduced should agree with that obtained from vertical sections intersecting tie line BE.

Checks should be made that there is consistency in the temperatures at which the liquidus surfaces for primary separation meet. In Figure 5b the temperature corresponding to point b should be higher than the temperature of point q in Figure 5c unless the monovariant curve e_1E passes through a temperature extremum. Authors sometimes present conflicting data, particularly when the ternary system contains pseudobinary sections. In Figure 7a the ternary system contains two pseudobinary eutectic sections, AB_2 - BC and A - BC, which divide the ternary system into three partial ternary

eutectic systems. A vertical section I - II, Figure 7b, is correct but a section such as Figure 7c is not. The temperature for intersection of the liquidus surfaces separating AB_2 and BC at point a is above the pseudobinary eutectic temperature for the system AB_2 - BC, represented by point b. Also the surface of secondary separation ab has an impermissible negative slope. Another trap to be wary of is the location of the intersection of surfaces of secondary separation on the invariant four-phase plane. With sparse experimental data, especially when the heat effect associated with secondary separation is not detected in a particular alloy composition, erroneous conclusion can be made. Figure 8 illustrates by full lines the true intersection point at c for the surfaces of secondary separation of AB_2 + BC and BC + B from the melt. The non-detection of a thermal effect for alloys d & c on the surface of secondary separation of BC + B led the author to select d as the intersection point. Had the author checked the consistency of intersection point d with intersection points on other vertical sections the error would have been apparent.

As tie lines and tie triangles are the basis of ternary equilibria it is often useful to check that stated compositions do lie on a straight line. One of the simplest methods is to calculate the equation of the tie line using as the basis the two most accurately determined compositions on the tie line. It will be recalled that the equation of a line between two points with coordinates $(x_1\ y_1)$ and $(x_2\ y_2)$ is:

$$y = x\left(\frac{y_2 - y_1}{x_2 - x_1}\right) + y_1 - x_1\left(\frac{y_2 - y_1}{x_2 - x_1}\right)$$

Having derived the equation of the tie line a check is made of the compositions of other points on the line for comparison with those given by the authors. The necessary amendments to compositions can then be made.

Authors may sometimes use mole fractions to represent compositions. If the components are the end members of a vertical section the mole fraction equals the atomic fraction. If the section is constructed between component A and component BC_2 and it is found that there is a eutectic at 0.18 mole fraction A and 0.82 mole fraction BC_2 the atomic fractions of A, B and C at the eutectic composition can be derived as follows:-

At the eutectic composition there are 0.18 mole A, 0.82 mole B and 2 x 0.82 mole C = 2.64 mole total.

The atomic fraction of A = $\frac{0.18}{2.64}$ = 0.0682 etc. The atomic % A is 6.82.

When compositions are given in mole fractions it is advisable to check that correct calculation of the atomic percentage has been made, since the ternary diagram will normally be scaled in atomic percent of components although a pseudobinary section involving a compound may have been expressed in mole fraction of the compound.

The pseudobinary sections shown in Figures 9 - 11 are incorrect and would not be accepted in any assessment, although they all appeared in journals with established refereeing procedures.

d Isothermal Sections

Many ternary systems have not been fully explored and frequently the literature contains one or two isothermal sections only. The majority have been determined by heat treating samples for a stated period and quenching to room temperature for determination of the phase structure. When studying low temperature equilibria some authors use insufficient heat treatment times and do not achieve equilibrium as evidenced by the reporting of more than three co-existing phases. A lot of detailed experimental work has been rendered useless by inattention to the need to equilibriate specimens.

Isothermal sections should show agreement of the ternary two-phase region boundaries with the equivalent binary data. The older ternary literature may not show agreement with modern binary data and in such cases it is necessary to adjust the ternary data. However, some ternary data has led to revisions of early binary data and it must not be assumed automatically that all binary data is of greater precision than ternary data.

If isothermal sections have been determined at a number of temperatures, preferably above and below each invariant reaction in the system, it is possible to construct the reaction scheme for the ternary. The main drawback of isothermal sections is that usually insufficient sections have been determined to allow any firm conclusions to be made on the reaction equilibria.

Certain rules govern the construction of isothermal sections. Frequently these rules are ignored in publications and it is necessary to adjust the data to conform with the following rules:-

1 three-phase regions appear as triangles,

Figures 12 - 14 show examples from published literature where three-phase regions are not represented correctly. In Figure 14 the $\beta_1 + \delta + \xi$ tie triangle is correct but the other three tie triangles are incorrect.

Figure 15 is an example of "tie triangles" with two corners only.

2 each tie triangle is associated with three two-phase regions,

3 each tie triangle makes contact at a vertex with a one-phase region,

4 if the boundaries of the one-phase region, touching a vertex of the tie triangle, are extrapolated the metastable extensions both lie inside the tie triangle or they lie on each side of the tie triangle in the two-phase regions. In Figure 16 constructions a) and b) are correct, c) and d) incorrect. Constructions from published work that illustrate incorrect constructions are shown in Figures 17 - 22. Errors of the type illustrated in Figure 16c are shown in Figure 17 (β^1 vertex of tie triangle $\alpha + \alpha_1 + \beta^1$), Figure 18 ($\beta$ vertex of $\alpha + \beta + \gamma$), Figure 19 (β vertex of $\alpha + \beta + \delta$) and Figure 20 (L_1 vertex of $L_1 + L_2 + C$). Figure 21 shows errors quoted in Figure 16c and 16d; the α vertex corresponds to Figure 16c and the γ vertex to Figure 16d. Figure 22 (α vertex of $\alpha + \beta + \beta_o$) and Figure 23 (γ vertex of $\gamma + \gamma^1 + \varepsilon$) are also examples of errors similar to Figure 16d.

5 tie lines in any two-phase region cannot cross.

e Designation of Phase Regions

One of the most useful approaches to the designation of phase regions in complex sections of ternary systems is due to Palatnik and Landau. They derived a general relationship for the dimension, R_1, of the boundary between neighbouring phase regions in a R-dimensional phase diagram or section of a phase diagram:

$$R_1 = R - D^- - D^+ \geqslant o$$

where D^- and D^+ represent, respectively, the number of phases that disappear and the number that appear in a transition from one phase region

to the other. The second rule, the cross rule, deals with the phase distribution in the four phase regions that meet at a point in two-dimensional sections or along a line (or at a point) in three-dimensional models of ternary phase diagrams. If the phase region with the minimum number of phases is designated $\alpha_1 + \alpha_2 + ... + \alpha_\lambda$ the opposite phase region contains the maximum number of phases, $\alpha_1 + \alpha_2 + ... + \alpha_\lambda + \alpha_{\lambda+1} + \alpha_{\lambda+2}$. Between these two phase regions are phase regions containing the phases $\alpha_1 + \alpha_2 + ... + \alpha_\lambda + \alpha_{\lambda+1}$ and $\alpha_1 + \alpha_2 + ... + \alpha_\lambda + \alpha_{\lambda+2}$.

These rules are useful for checking phase designations in vertical and isothermal sections. In Figure 24 the phase regions adjoining the liquid phase region are correctly designated. Similarly the phase regions at the horizontal invariant line, represented as a degenerate phase region of $L + \alpha + \beta + \gamma$, are correctly designated for the $L + \beta$ end of the horizontal. At the other end of the invariant horizontal the authors inserted an undesignated phase region. The existence of this phase region, denoted by a question mark, is not possible. The phase boundary that slopes down to the invariant reaction $\alpha + \beta \rightleftharpoons \gamma + \delta$ is an impossible construction. The $\alpha + \gamma$ phase region extends to both invariant horizontals. In Figure 25a the diagram as presented did not conform with the known phase relations for component B. The $L + \gamma$ phase region was shown as stable over too wide a temperature range; the necessity for an $\alpha + \gamma$ phase region in the section was solved by inserting a second $L + \alpha + \gamma$ phase region between the $L + \gamma$ and the $\alpha + \gamma$ phase regions. This led to an unacceptable meeting of boundaries at the B component for the reaction $\alpha + \gamma \rightleftharpoons \beta$. The acceptable section is shown in Figure 25b.

It is always advisable to check the designation of phase regions in published work. In complex ternary systems it can be difficult to assign the correct phases to each region, apart from the occasional printer's errors. When vertical sections are given for say constant % A and constant % C a check should be made that the thermal arrests for the alloy whose composition falls on both sections are plotted in the same way on both sections and that the sequence of phase regions associated with the alloy on cooling from the melt is the same in each section.

The critical assessment of ternary alloy phase diagram data is not divided into the five sections dealt with in this paper. All the data is assessed as a continuing process and not in isolation. The end result should be the presentation of consistent data which the reader may use with confidence. If the basic data does not allow the achievement of this objective the attention of the reader should be drawn to areas of uncertainty and a statement made of the further work needed to clarify the equilibria.

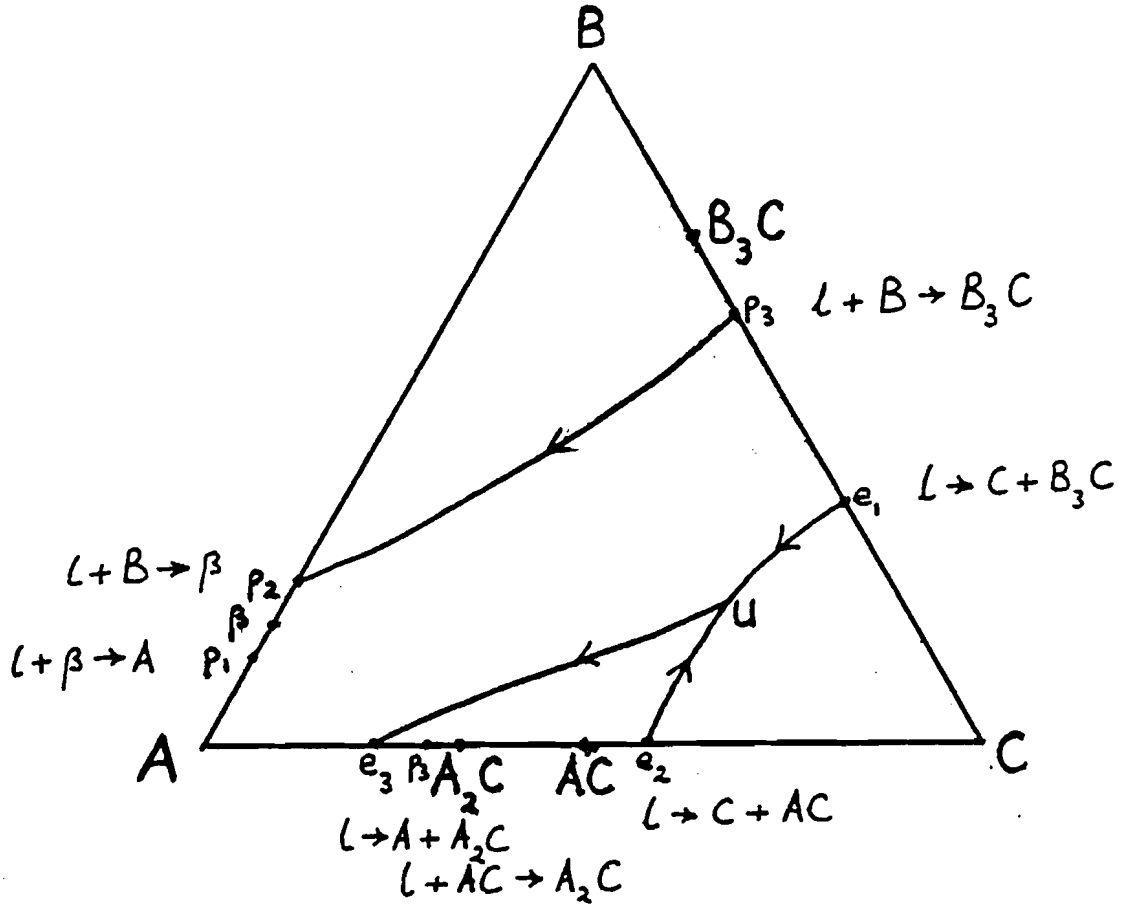
B
B3C
p3
L + B → B3C
e1
L → C + B3C
L + B → β
p2
β
L + β → A
p1
u
A
e3
β
A2C
AC
e2
C
L → A + A2C
L + AC → A2C
L → C + AC

1

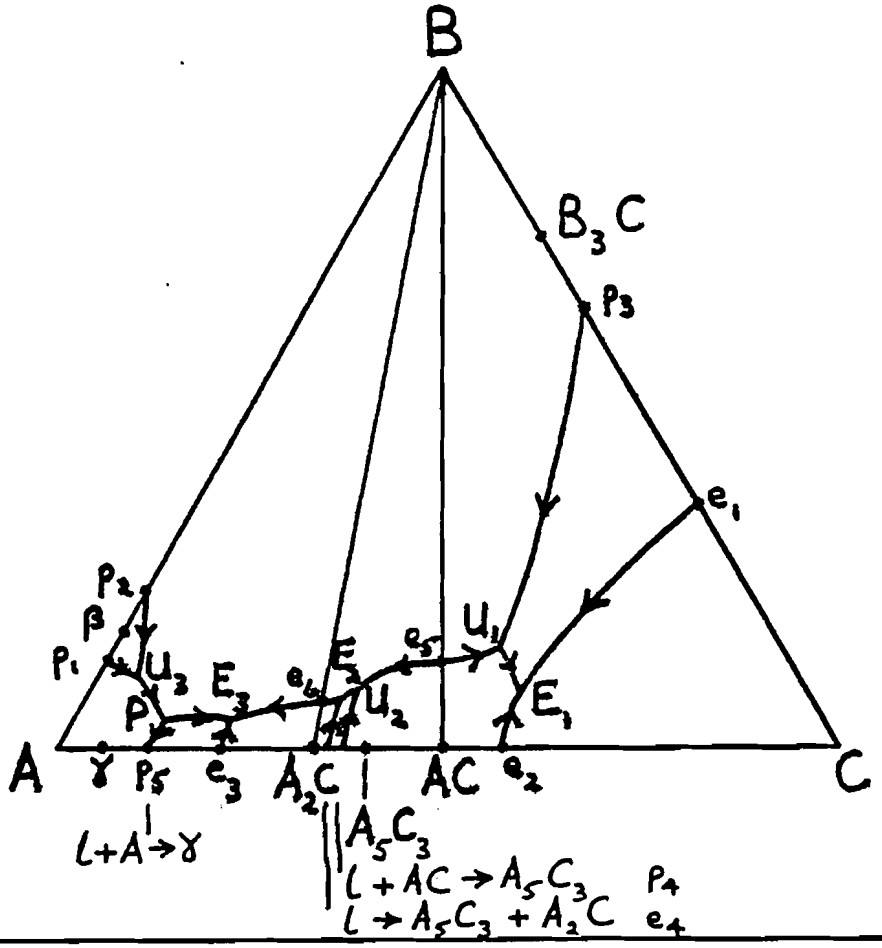
B
B3C
p3
e1
p2
β
p1
U3
E3
e6
P
U2
e5
U1
E2
E1
A
γ
p5
e3
A2C
AC
e2
C
L + A → γ
A5C3
L + AC → A5C3
P4
L → A5C3 + A2C
e4

2

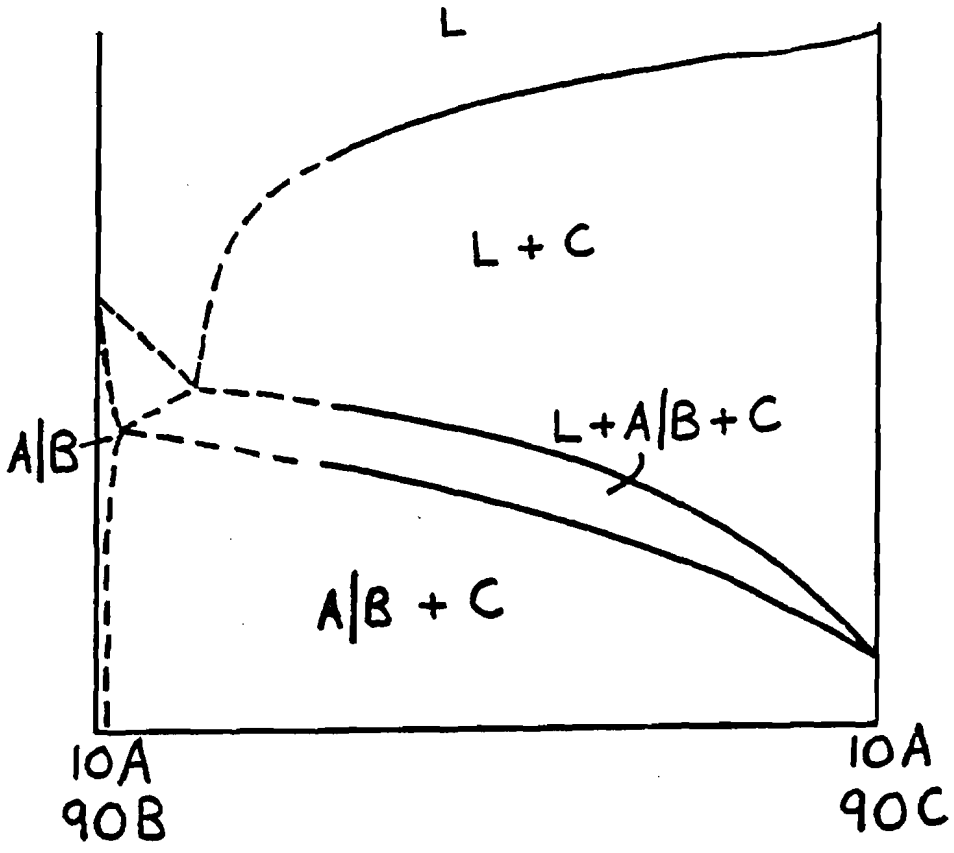

a

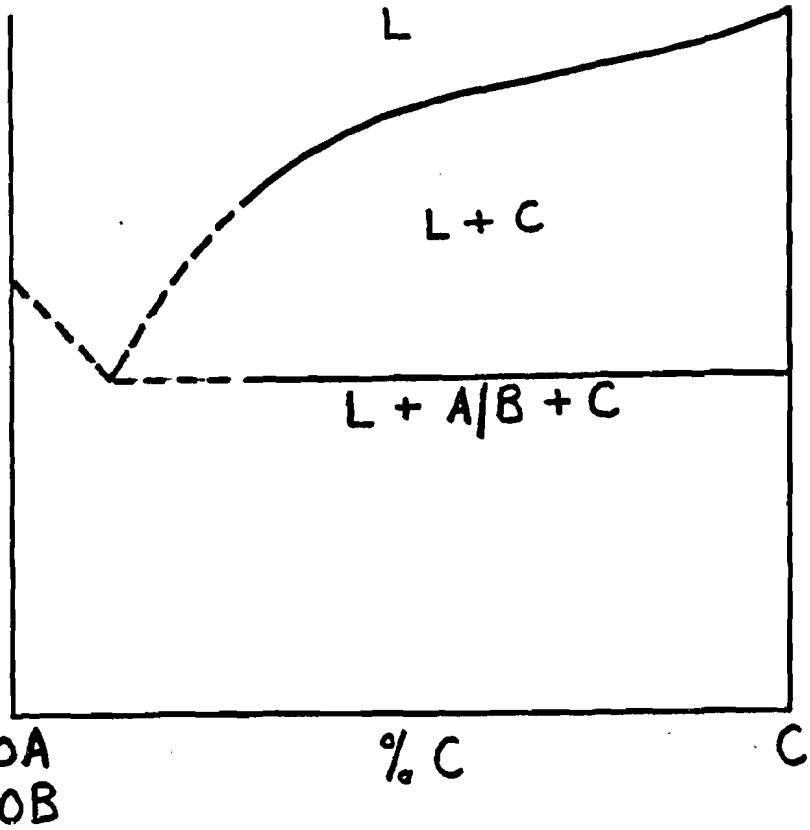

b

S&C
HRC

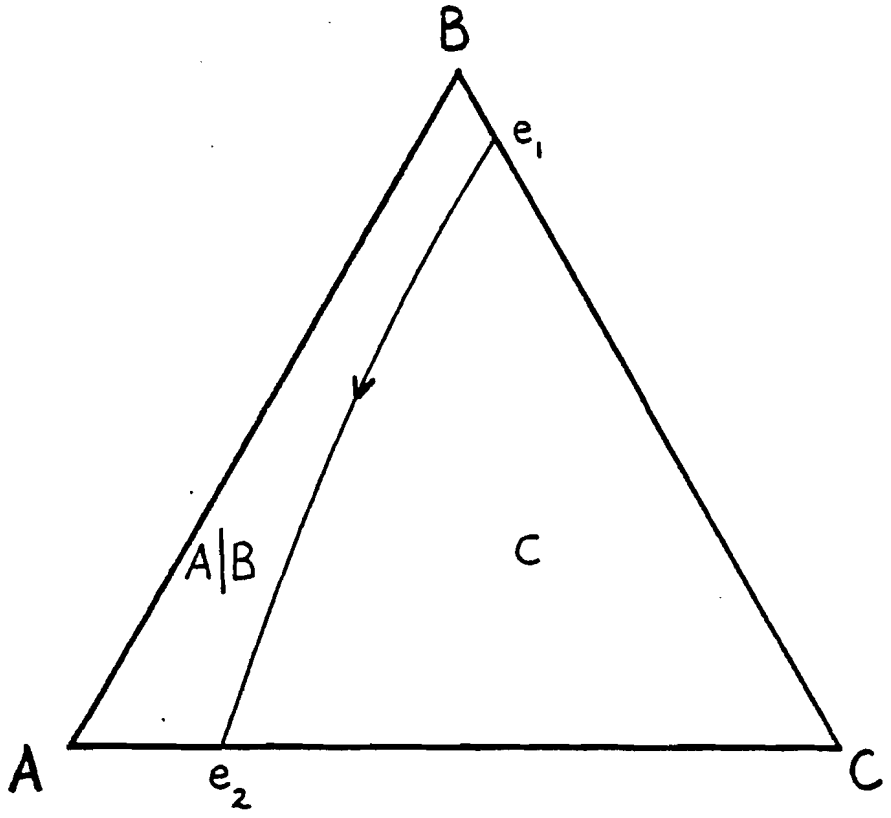

GEC
HRC

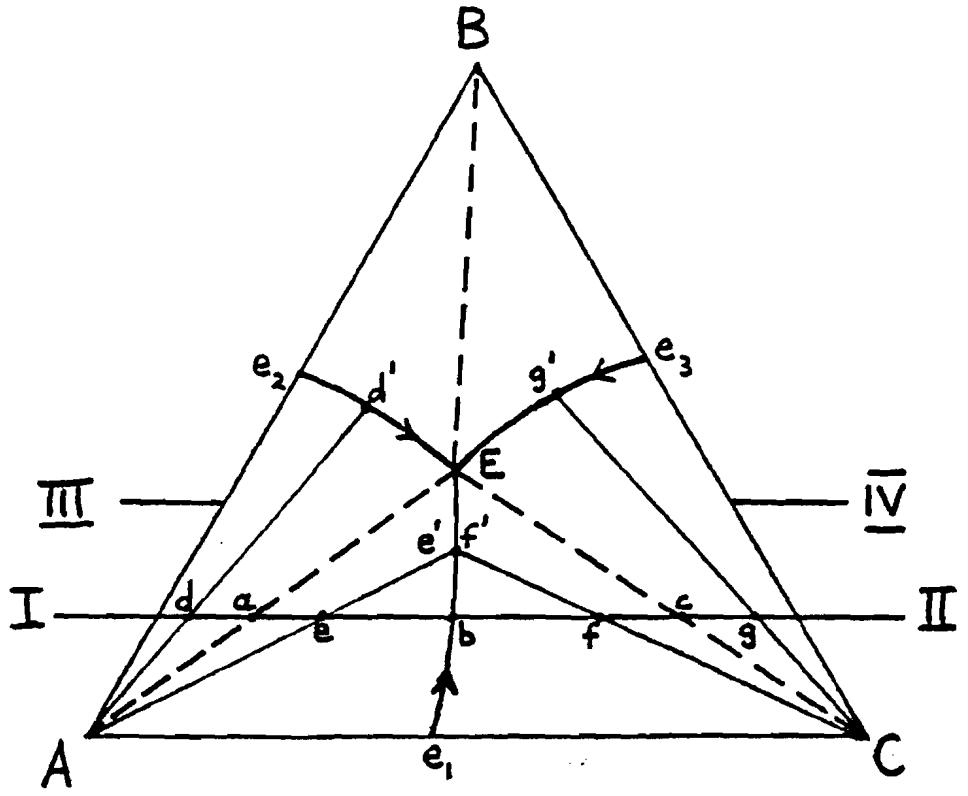
B
A
C
E
e1
e2
e3
d'
g'
e'
f'
III
IV
I
II
d
a
e
b
f
c
g

a

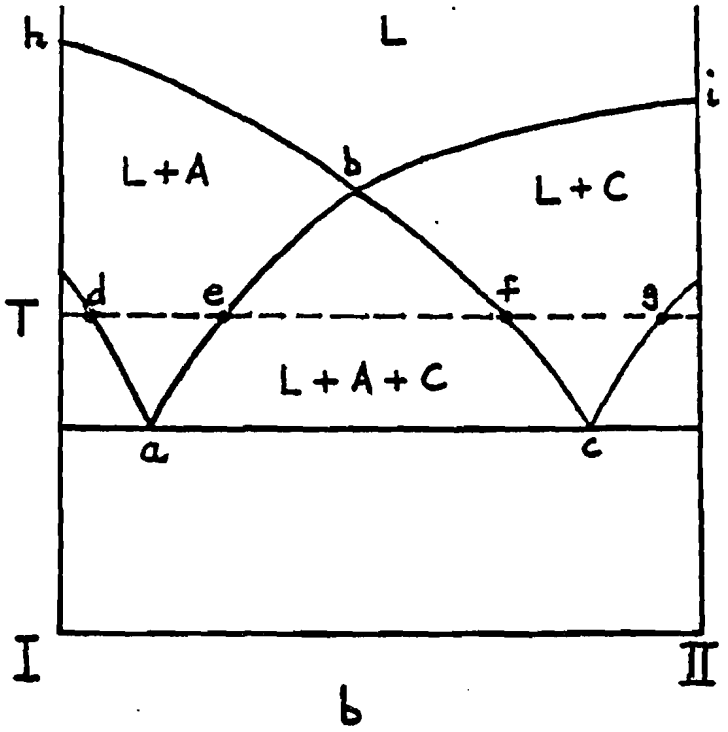
h
L
i
L+A
b
L+C
T
d
e
f
g
L+A+C
a
c
I
II

b

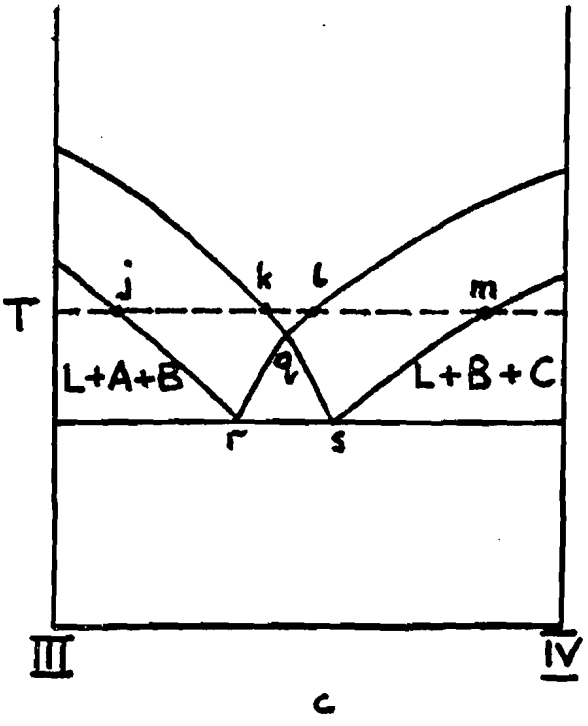
T
j
k
l
m
L+A+B
q
L+B+C
r
s
III
IV

c

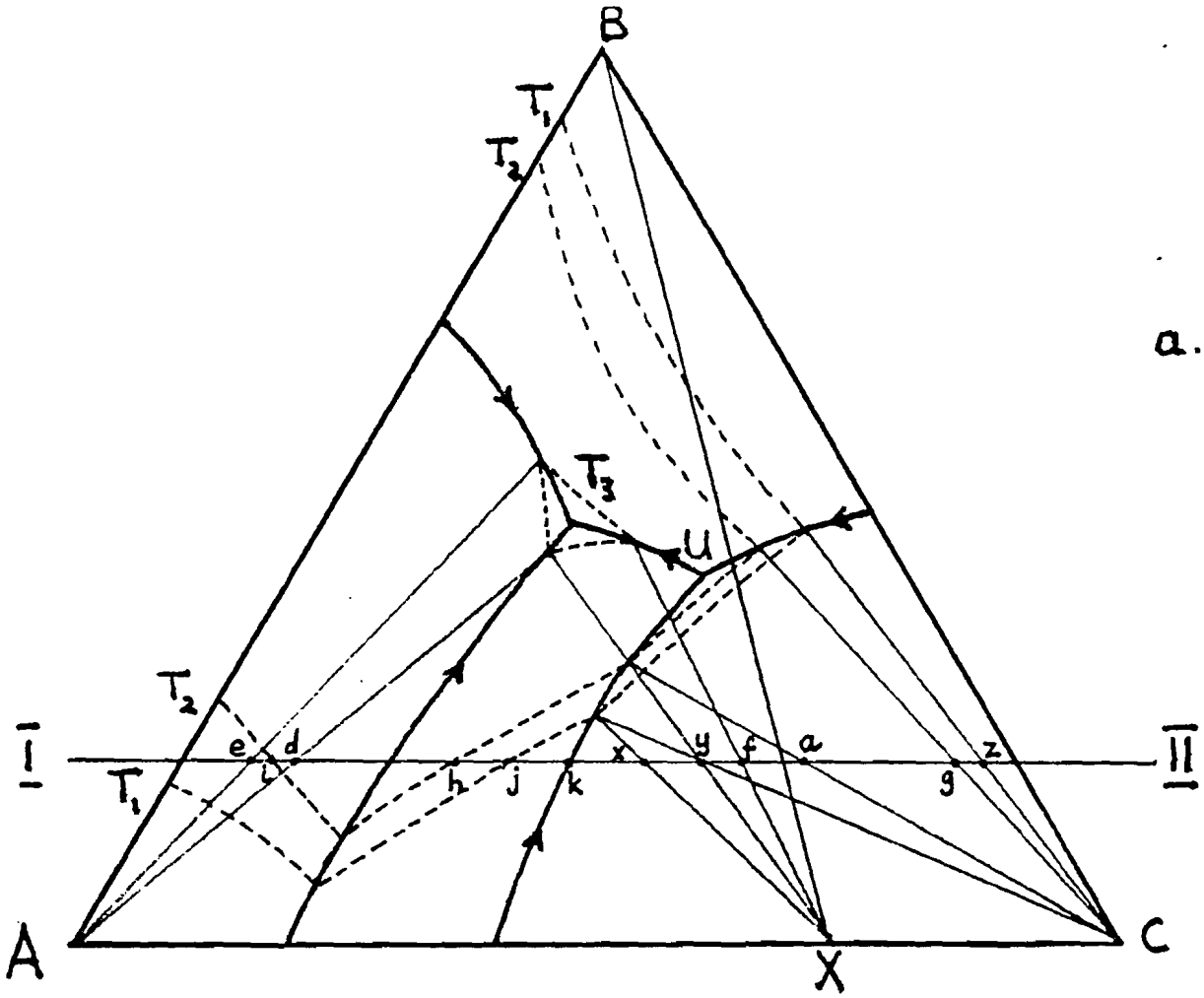
B
T1
T2
T3
U
T2
T1
I
II
e
d
h
j
k
x
y
f
a
g
z
A
X
C

a.

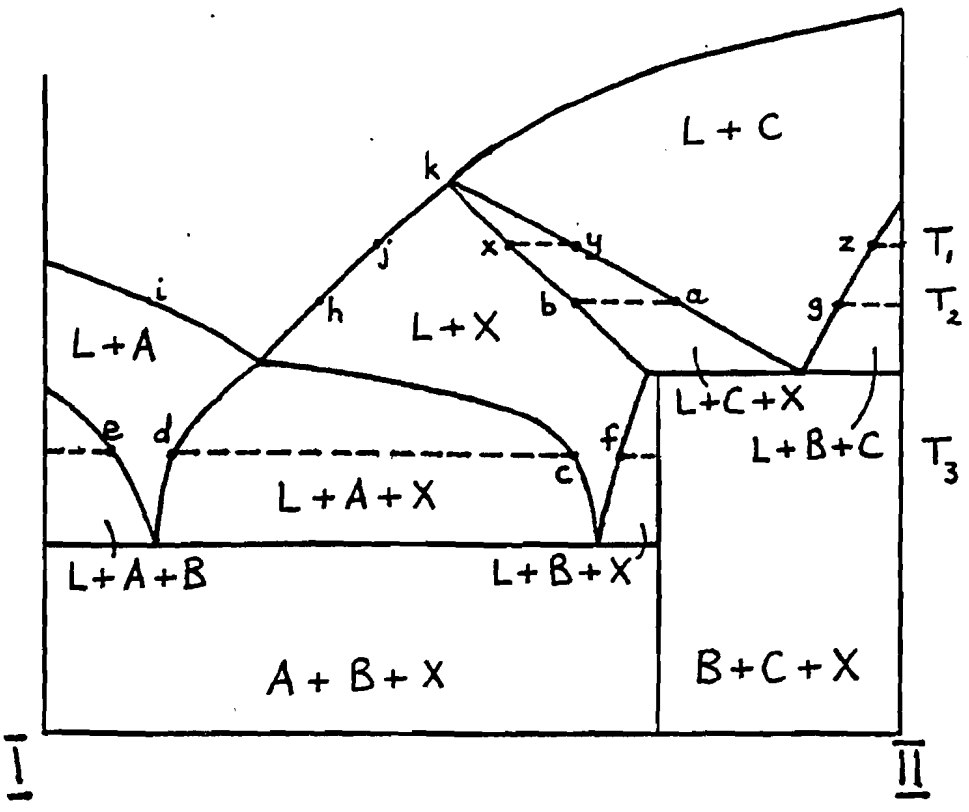
L + C
k
j
x
y
z
T1
i
h
b
a
g
T2
L+A
L+X
L+C+X
e
d
f
L+B+C
T3
c
L+A+X
L+A+B
L+B+X
A + B + X
B+C+X
I
II

b

S&C
HRC

b

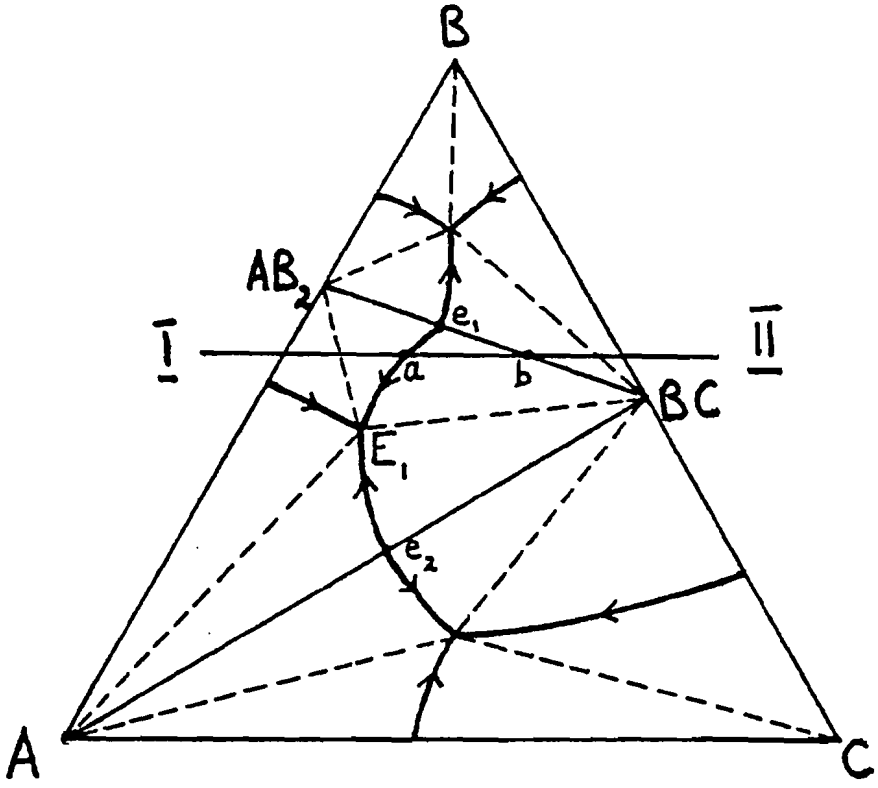

a

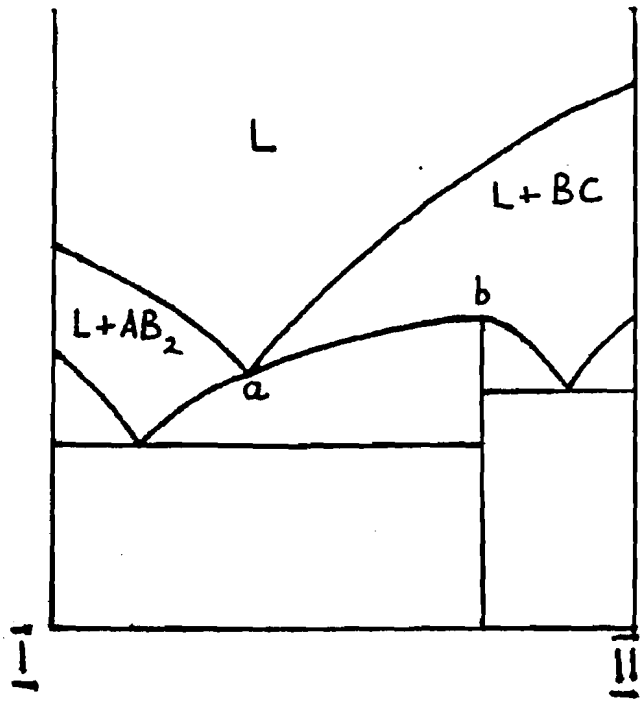

b

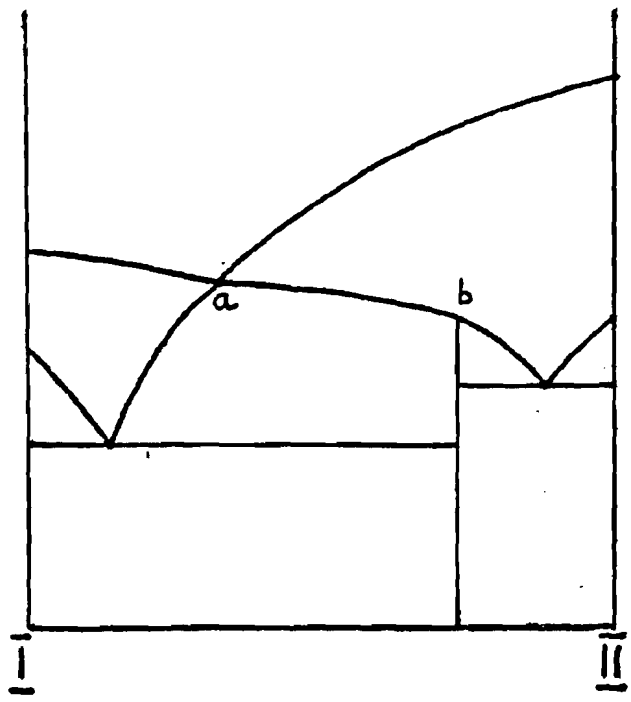

c

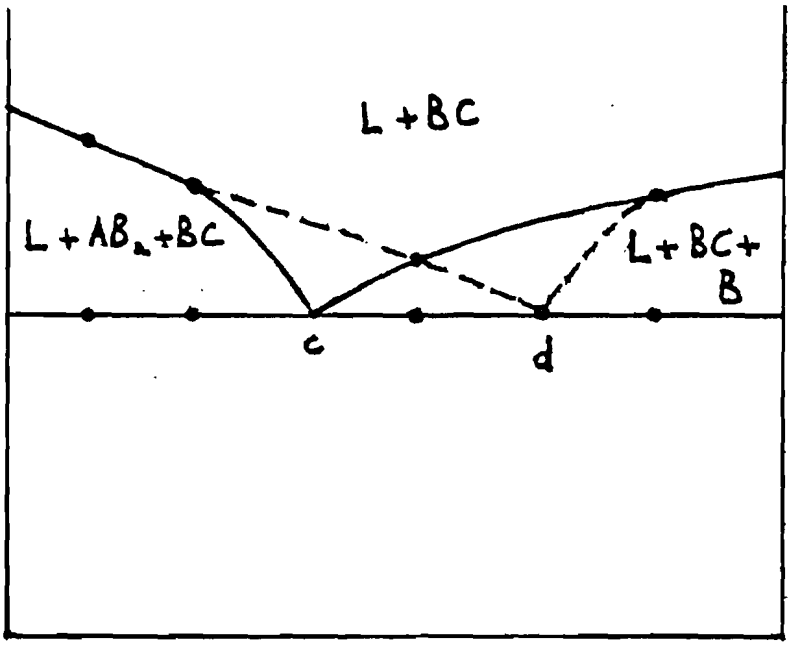

FIG . 9

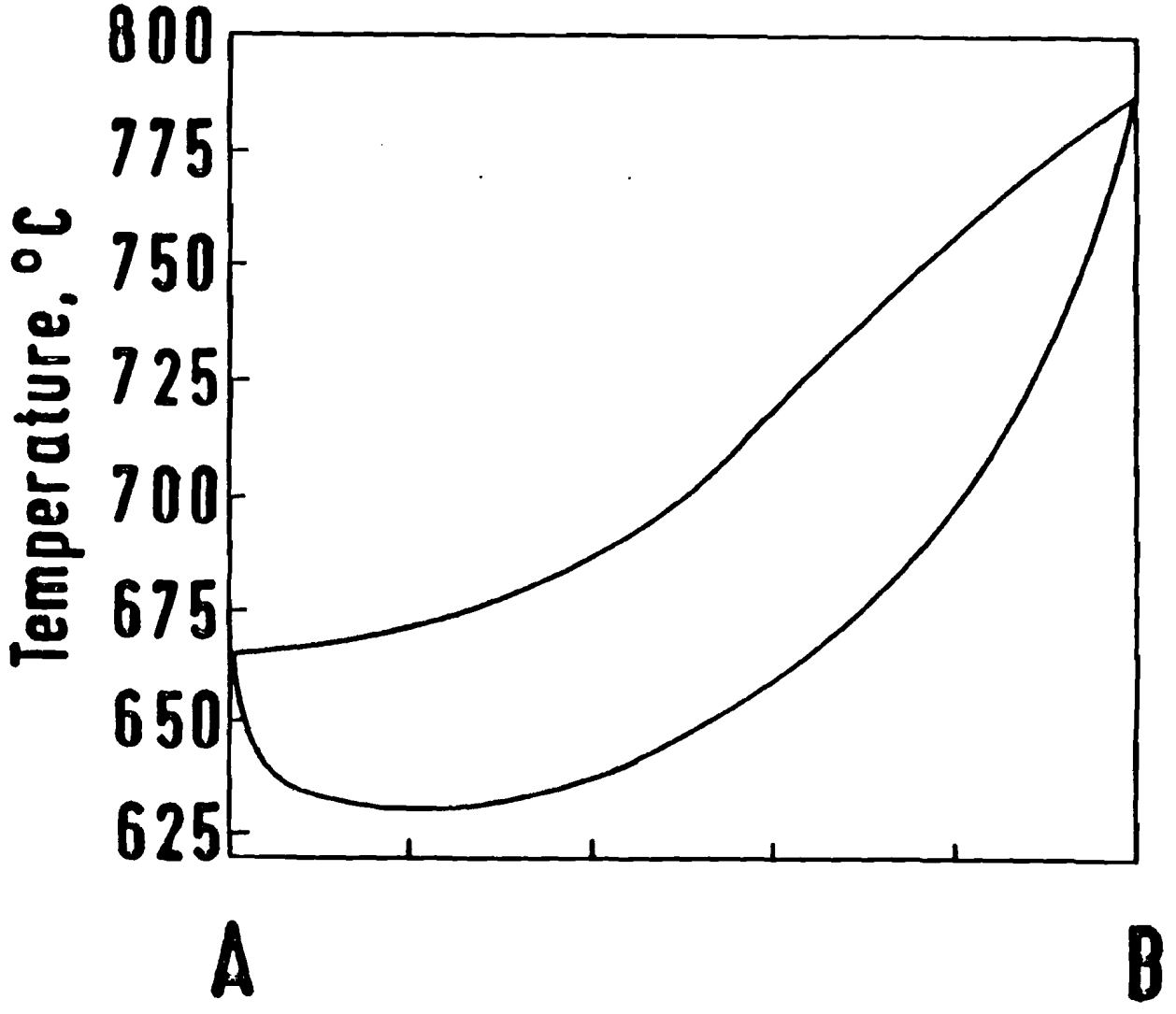

FIG. 10

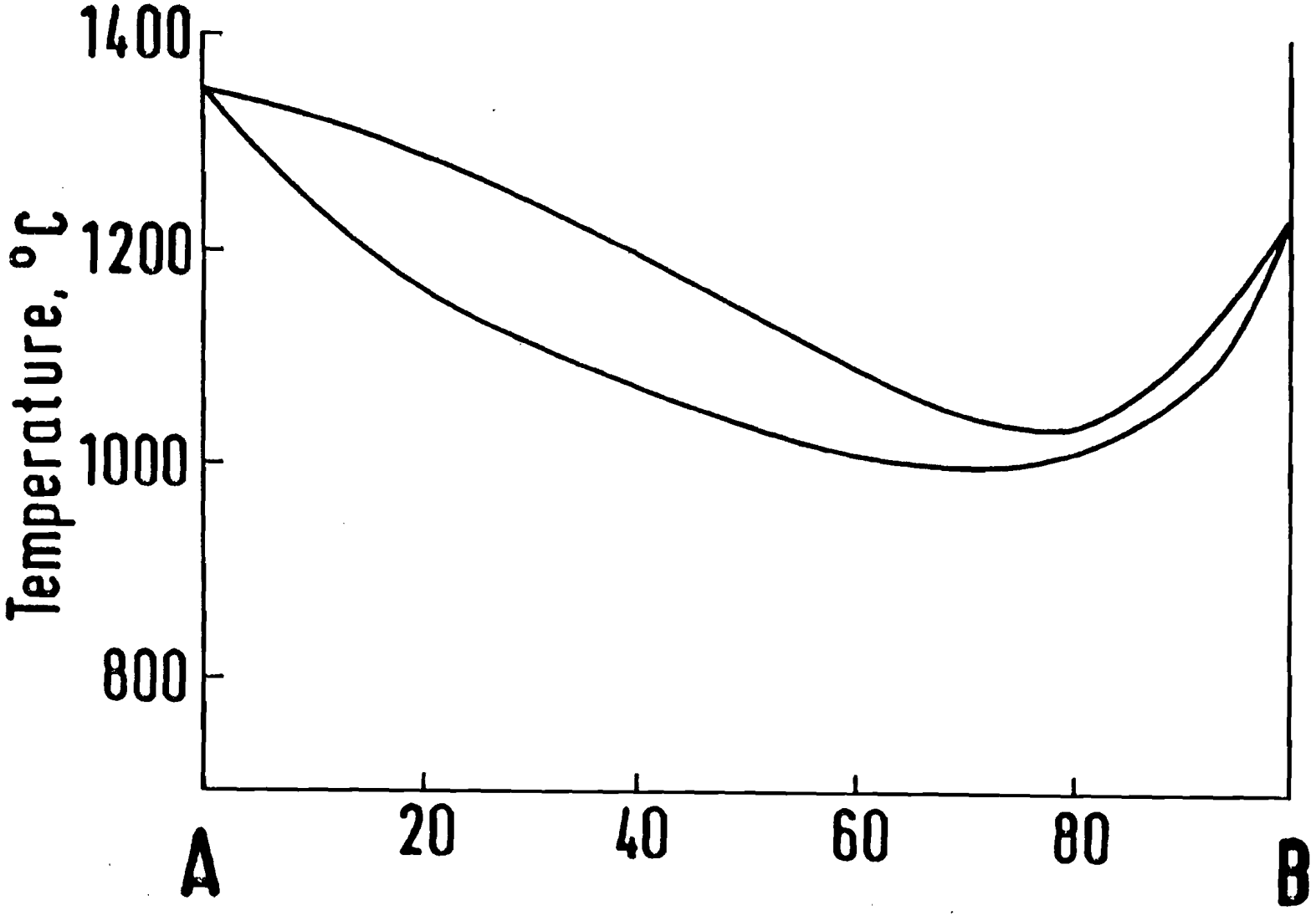

FIG . 11

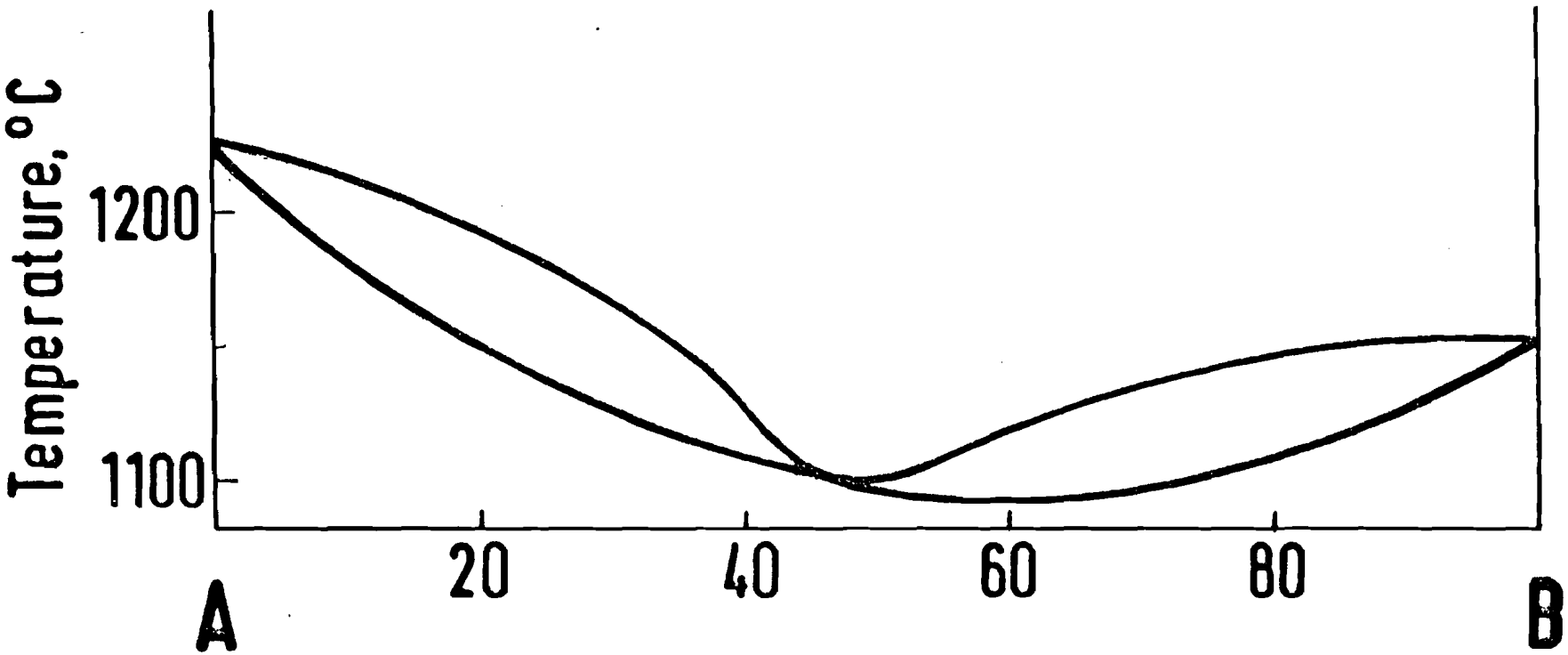

FIG. 12

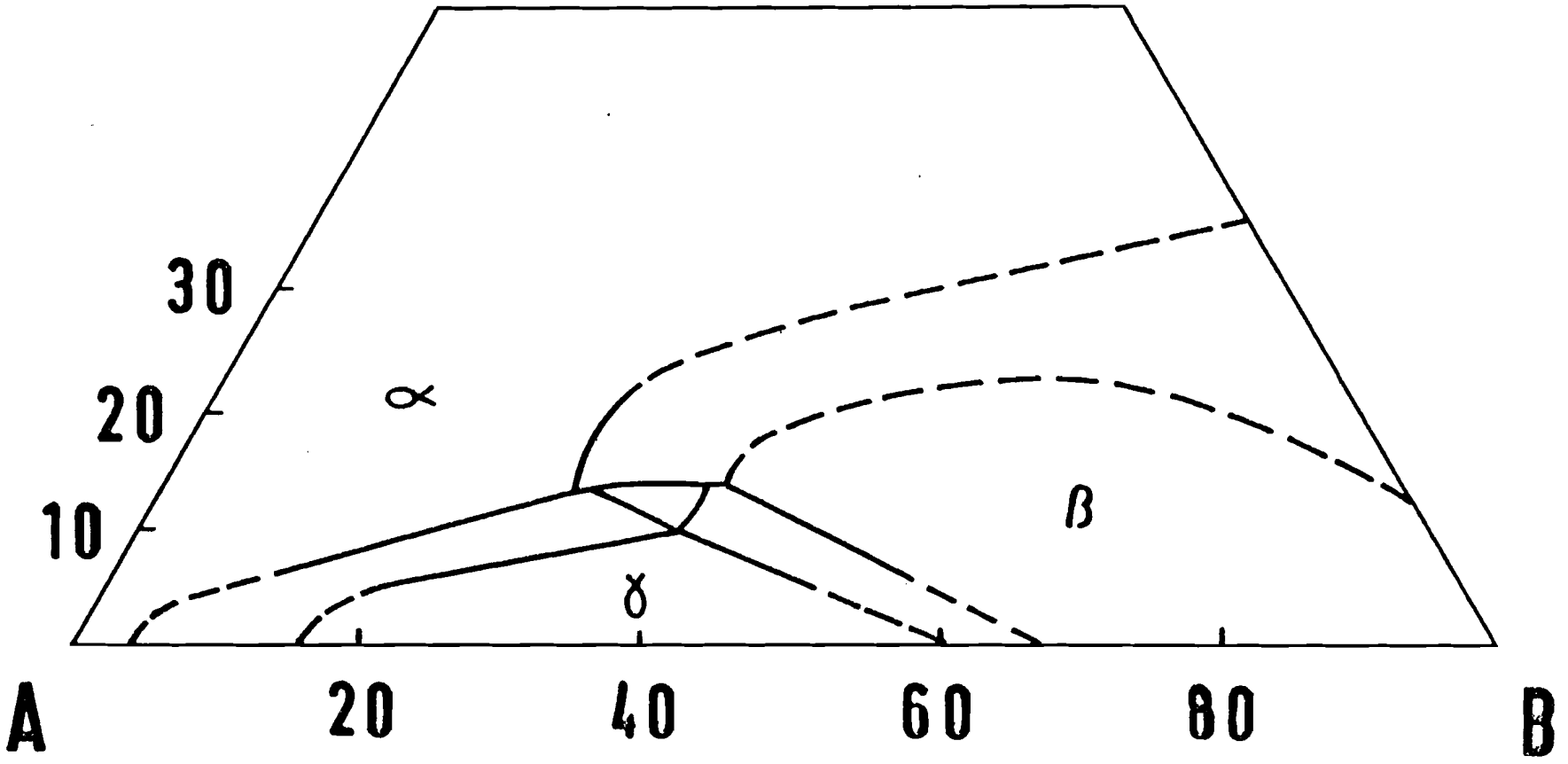

FIG .13

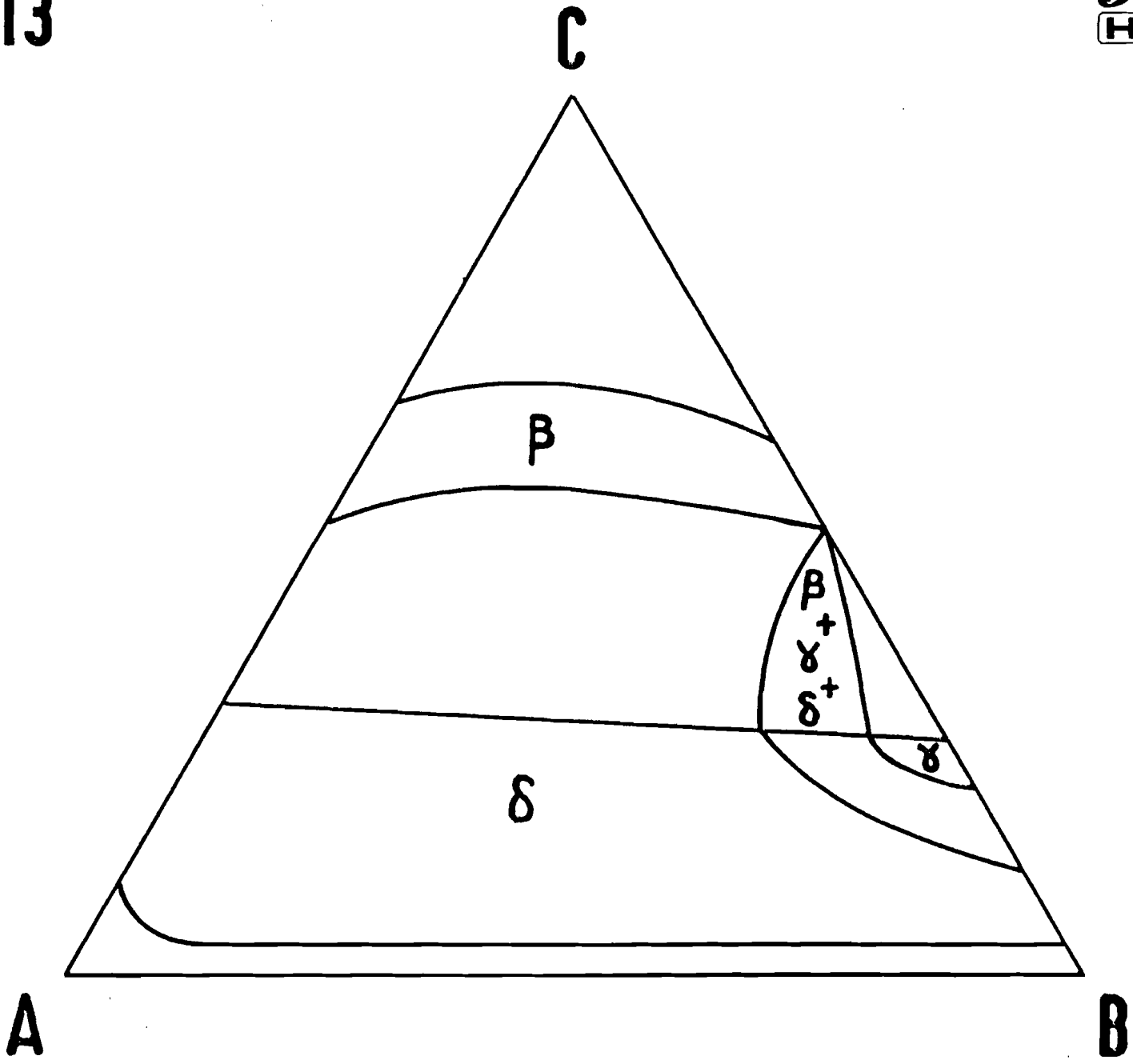

FIG .14

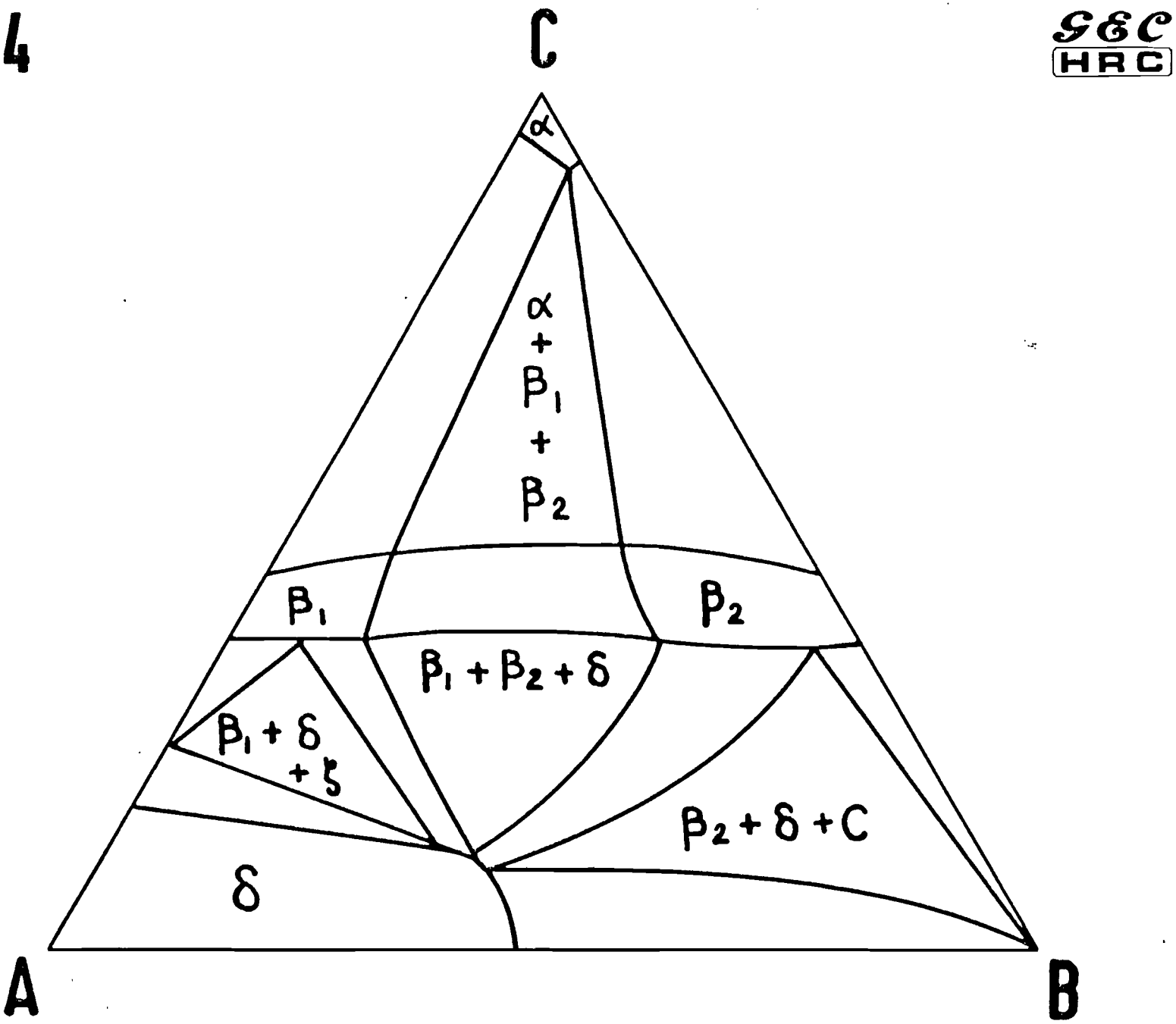

FIG .15

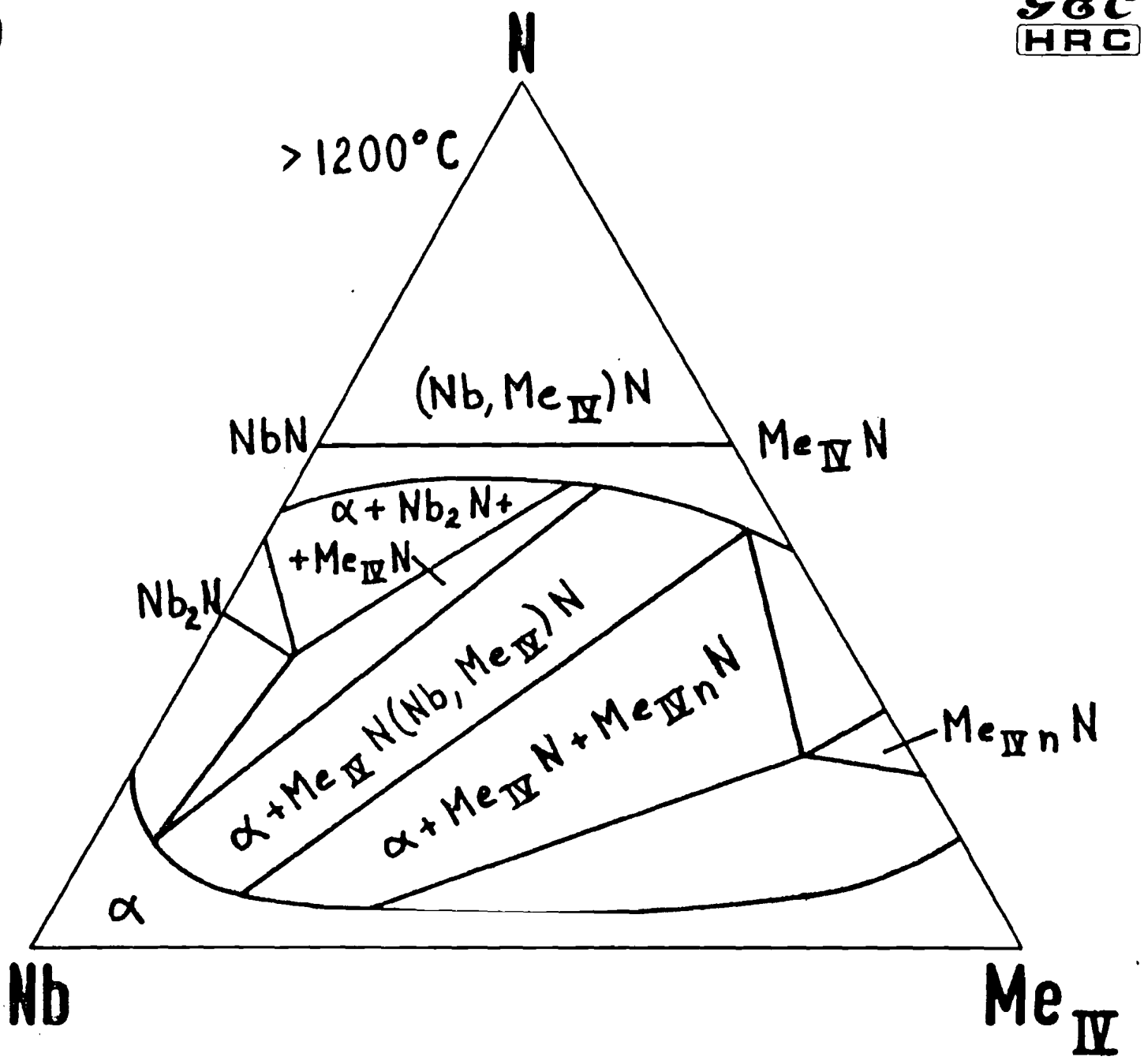
N
>1200°C
(Nb, Me IV) N
NbN
Me IV N
α + Nb2 N +
+ Me IV N
Nb2 N
α + Me V N (Nb, Me IV) N
α + Me IV N + Me IV n N
Me IV n N
α
Nb
Me IV

a

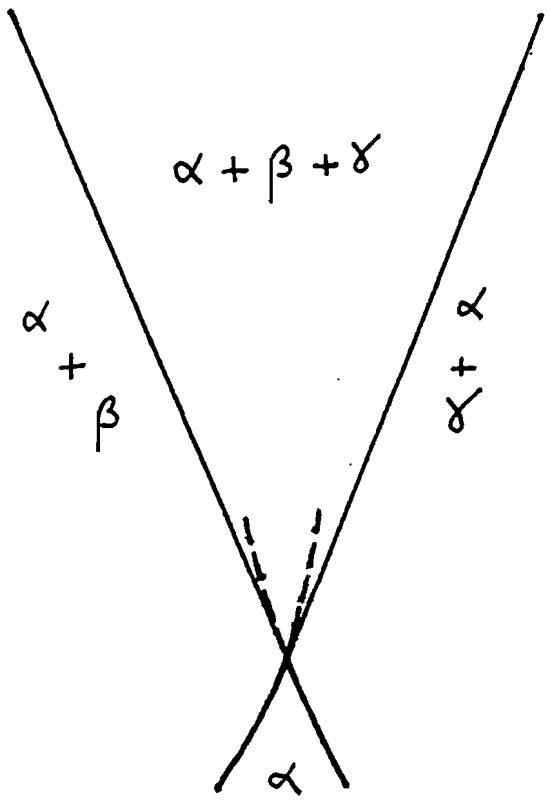

b

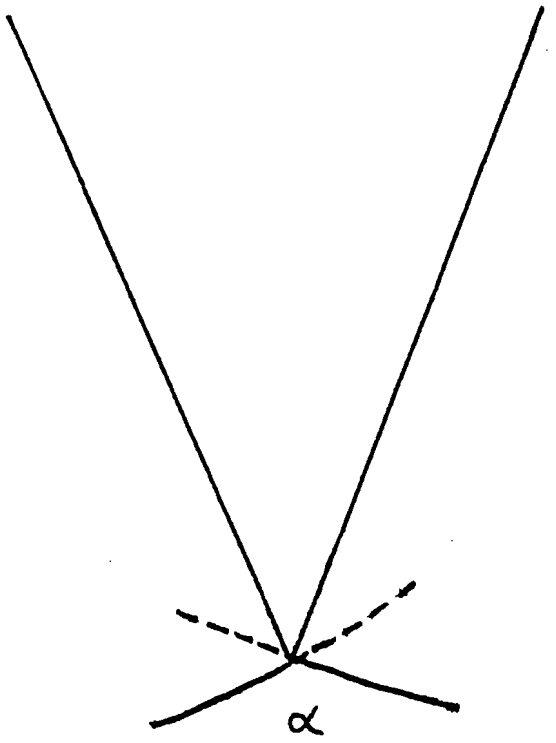

c

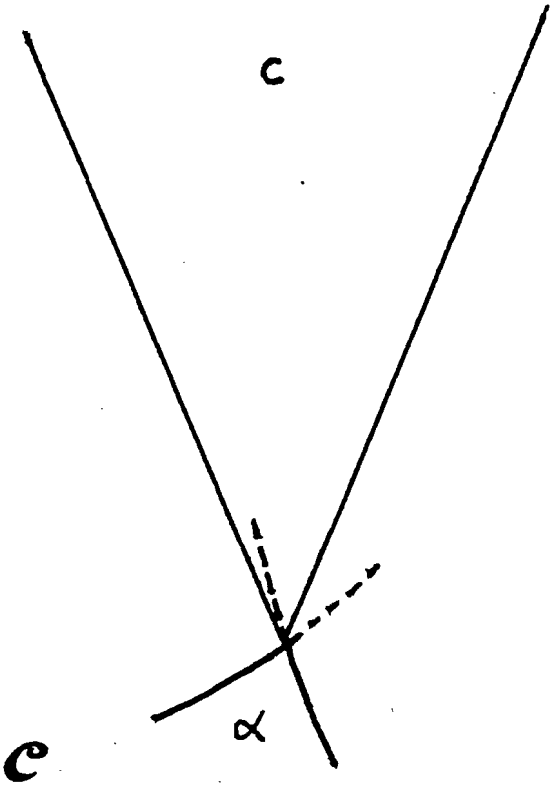

d

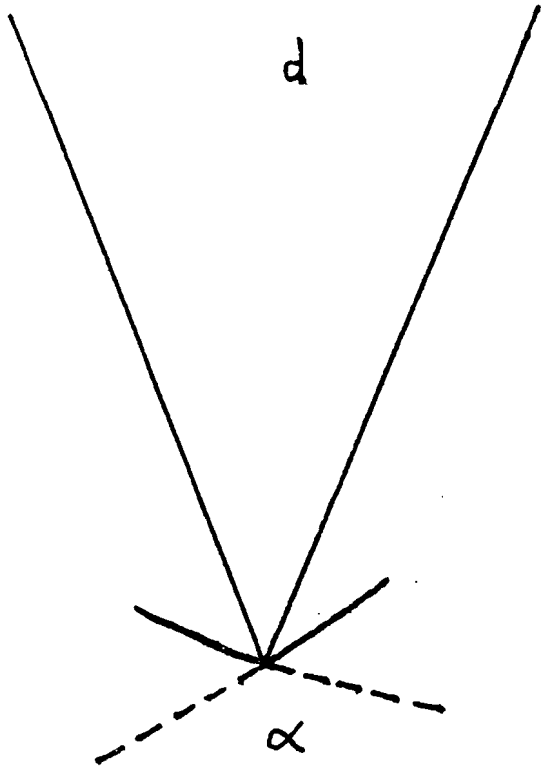

GEC HRC

FIG .17

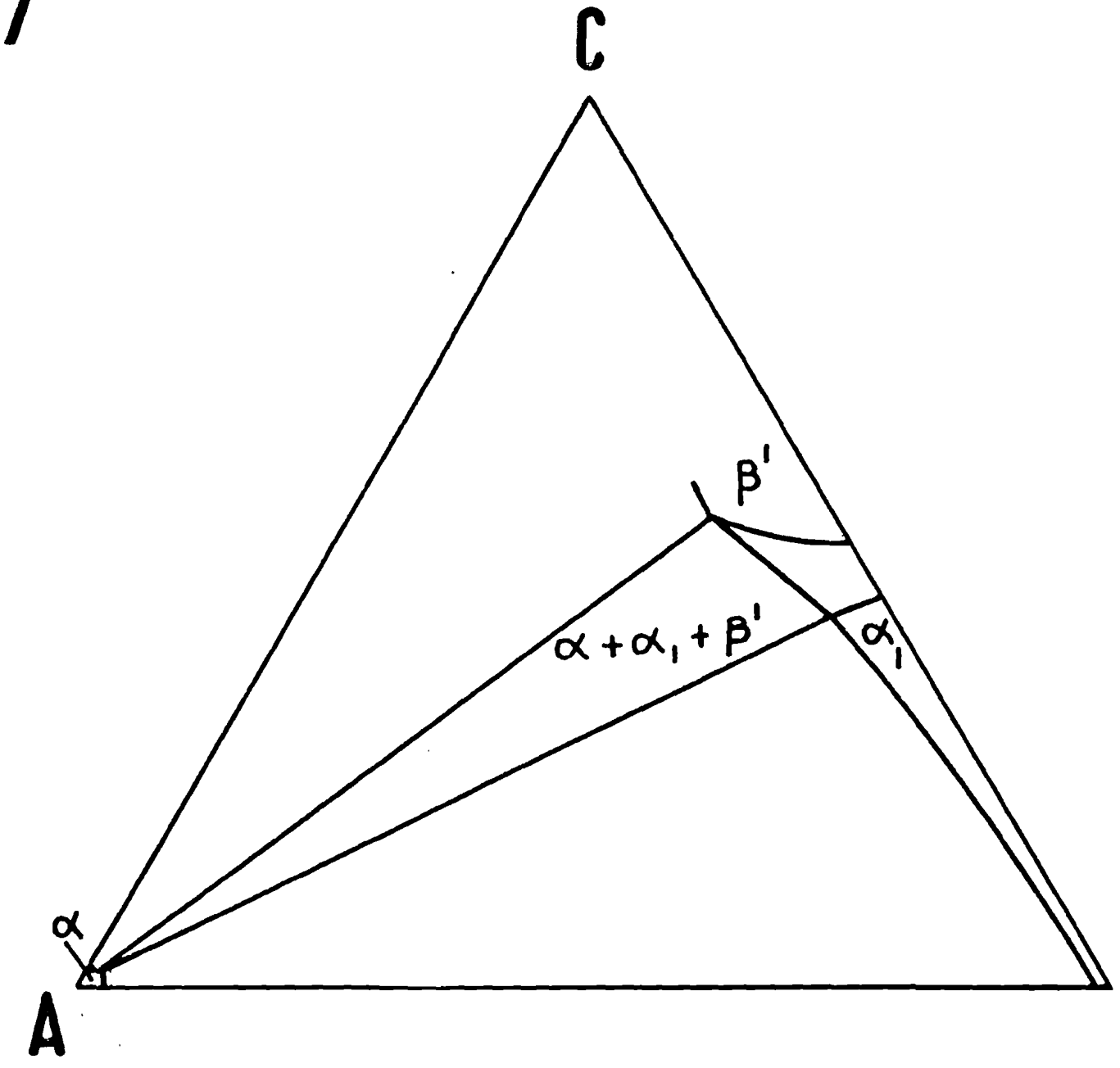

FIG. 18

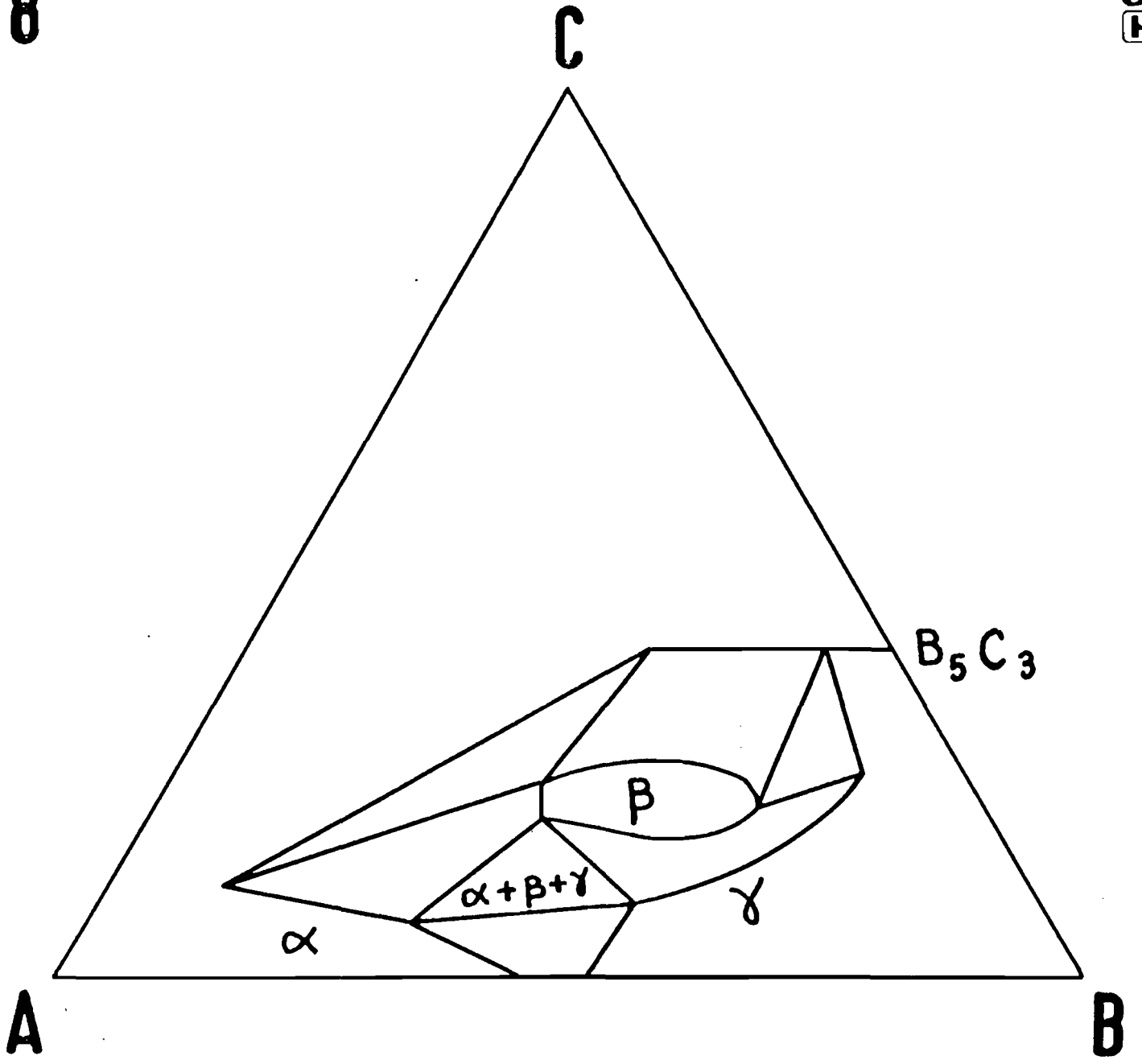

FIG .19

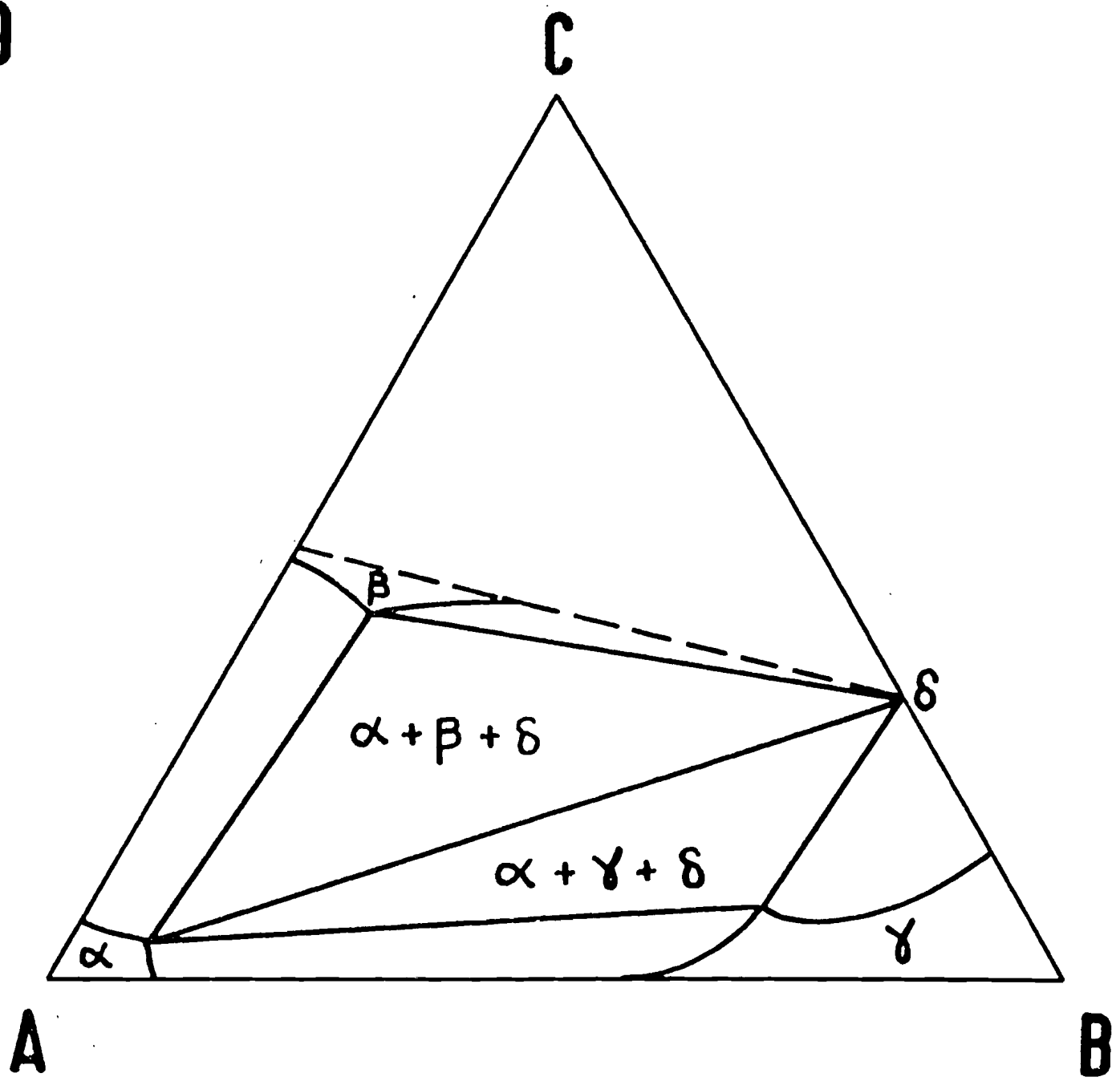

FIG . 20

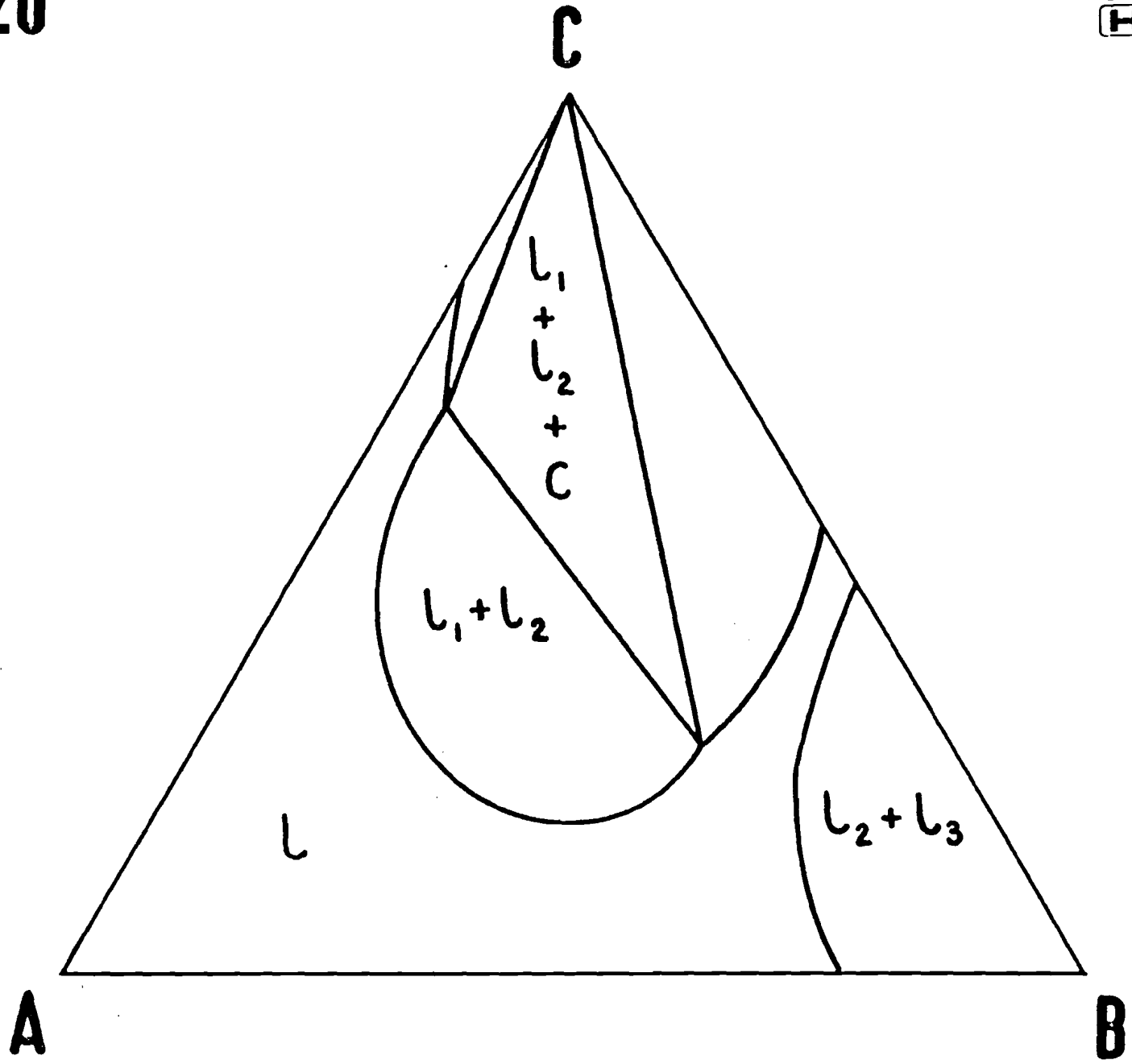

FIG . 21

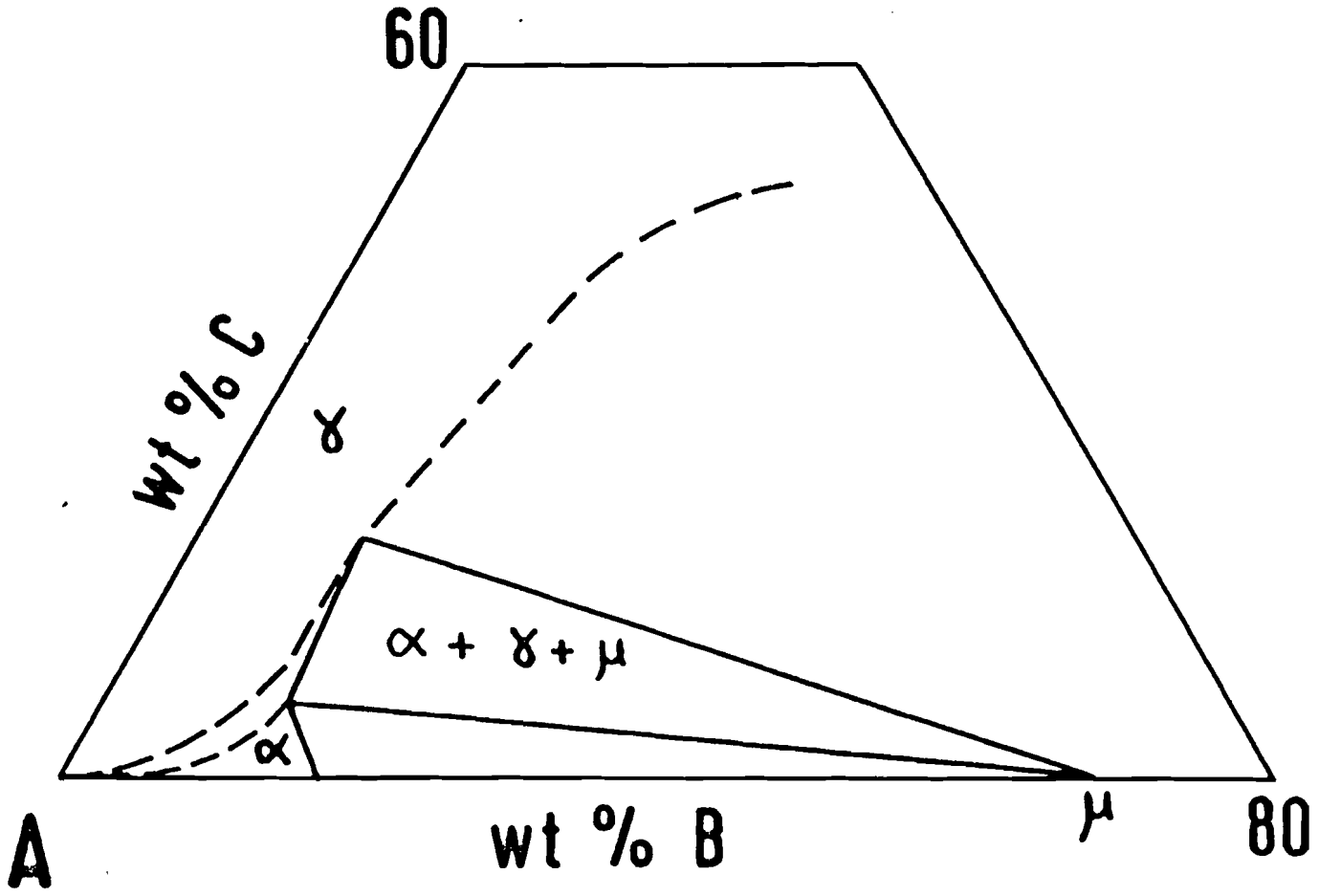

FIG . 22

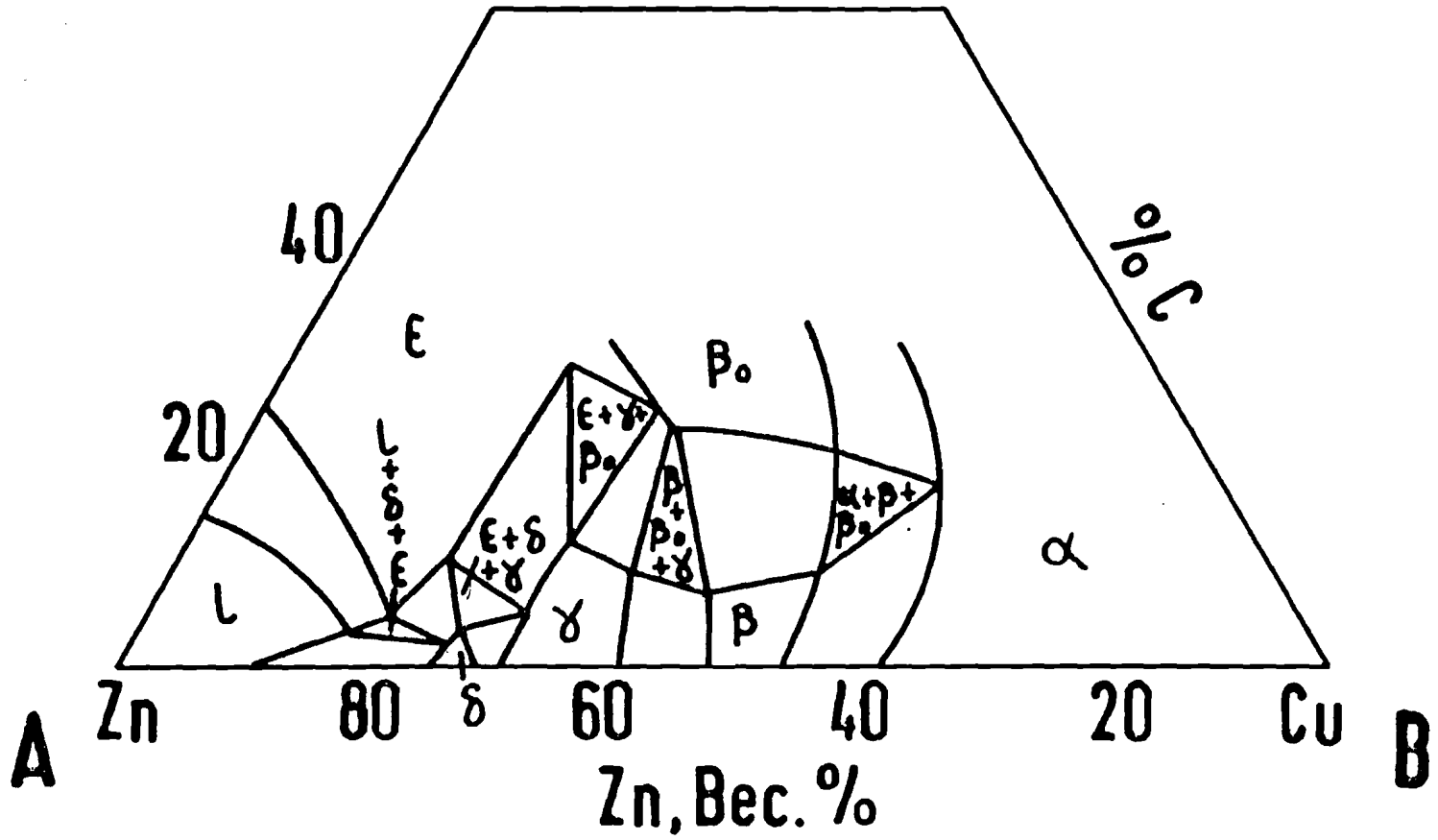

FIG. 23

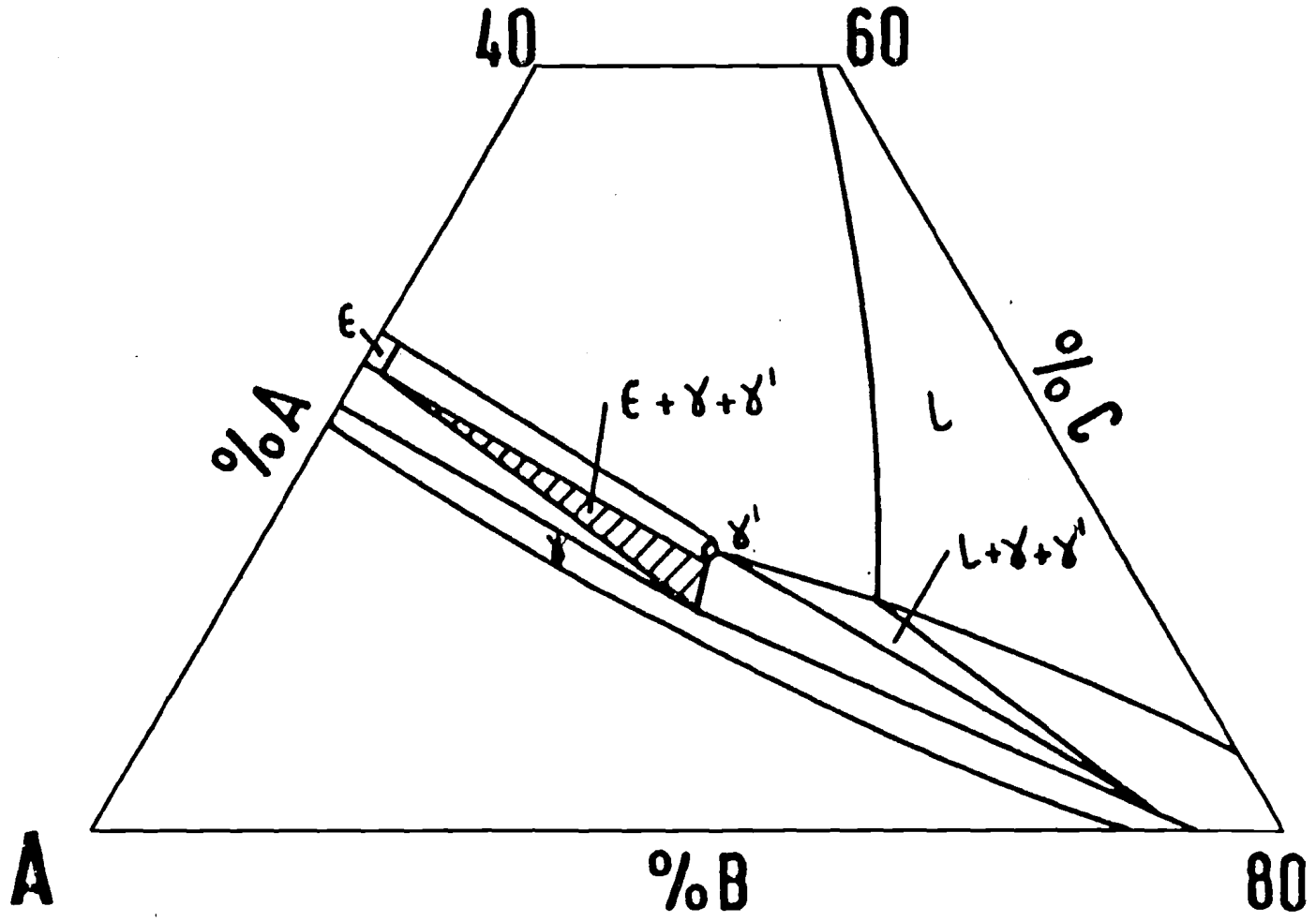

FIG . 24

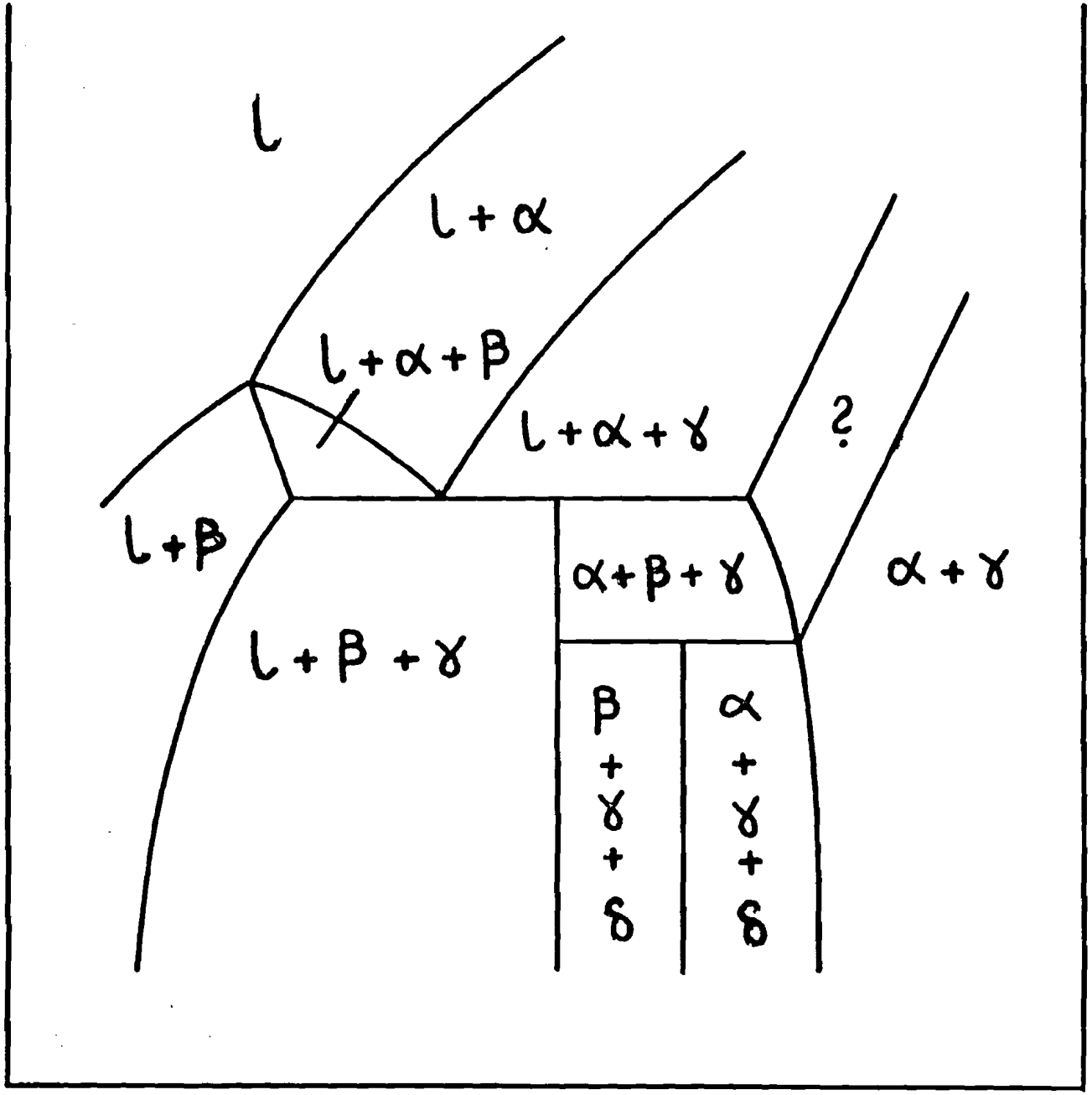

$L + \alpha \rightarrow \beta + \gamma$

$\alpha + \beta \rightarrow \gamma + \delta$

FIG. 25

SGC HRC